Coupling EDYS and TELEMAC-2D for Ecohydrological and Hydrodynamic Simulation of San Antonio Bay

by

Cade Coldren, Alireza Asadi, Ted Cleveland, and Ken Rainwater

Texas Tech University

Lubbock, Texas

Submitted to

San Antonio River Authority

100 East Guenther Street

San Antonio, Texas

August 2020

Table of Contents

List of Tables ii
List of Figures ii
Abstract… v
Acknowledgements v
1 Introduction 1
2 TELEMAC-2D Model 2
2.1 San Antonio Bay Application 2
2.2 Data Requirements 3
2.2.1 Model Domain 4
2.2.2 Boundary Conditions 4
2.2.3 Hydrologic Variables 5
2.2.4 Salinity Data 7
2.3 TELEMAC-2D Model Settings 8
2.3.1 Physical Parameters 8
2.3.2 Numerical Scheme 8
2.3.3 Tracer Calculations 9
2.4 TELEMAC-2D Preliminary Applications 9
3 Hydrodynamic Scenario Simulations 15
4 Linkage of EDYS with TELEMAC-2D 26
4.1 Domains and Linkage Steps 26
4.2 Measures for Comparison 28
5 Vegetative Responses to Hydrological Changes 28
5.1 Scenario 2 28
5.2 Scenario 3 30
5.3 Scenario 4 30
5.4 Scenarios 5, 7, and 9 32
5.5 Scenarios 6, 8, and 10 32
6 Conclusions 35
6.1 Scenario Simulations with the Ecohydrological and Hydrodynamic Models 35
6.2 Completion of Project Scope of Work 38
6.3 Thoughts for Future Applications 38
7 References 39
Appendices 41
A. Plant species simulated in the EDYS model application for San Antonio Bay 42
B. Community responses and individual plant species responses to additional releases during drought periods 44

List of Tables

1. Salinity Observation Stations....11
2. Scenarios for Coupled TELEMAC-2D and EDYS Simulations....16
3. Mean Spatial Extents of Vegetative Responses for Scenario 2....30
4. Mean Spatial Extents of Vegetative Responses for Scenario 3....30
5. Mean Spatial Extents of Vegetative Responses for Scenario 4....32

List of Figures

1. General location of the solution domain for the SA Bay model....3
2. Finite element mesh with 1664 nodes and 2689 triangular elements....5
3. TELEMAC-2D initial boundary nodes, with 27 freshwater inflow nodes (red), 50 TxBLEND tidal nodes (green), 491 runoff nodes (gold), and 520 no-flow nodes (blue)....6
4. Location of Aransas County Airport relative to SA Bay model....7
5. Simulated depth distribution for 12:00 a.m. July 29, 2005....10
6. Simulated salinity distribution for 12:00 a.m. July 29, 2005....10
7. Locations of salinity observations....11
8. Comparison of nearest model node location to ANWR monitoring site....12
9. Comparison of nearest model node location to Mesquite Bay monitoring site....12
10. Comparison of nearest model node location to Seadrift monitoring site....13
11. TELEMAC-2D simulation and observed data at ANWR monitoring site....13
12. TELEMAC-2D simulation and observed data at Mesquite Bay monitoring site....14
13. TELEMAC-2D simulation and observed data at Seadrift monitoring site....14
14. Scenario 2 diversion....17
15. Scenario 3 diversion and scenarios 5, 7, and 9 additions....17
16. Scenario 4 diversion and scenarios 6, 8, and 10 additions....18
17. Guadalupe River flows around the 1988-89 drought....19
18. Guadalupe River flows around the 1995-96 drought....19
19. Guadalupe River flows around the 2000-01 drought....19
20. Guadalupe River flows around the 2008-09 drought....20
21. Guadalupe River flows around the 2011-13 drought....20
22. Freshwater inflow locations for scenarios 1, 4, 6, 8, and 10....21
23. Freshwater inflow locations for scenario 2....21
24. Freshwater inflow locations for scenarios 3, 5, 7, and 9....22
25. Salinities for scenarios 1, 2, 3, and 4 at node near Seadrift....22
26. Depths for scenarios 1, 3, 5, 7, and 9 near mouth of Townsend Bayou, 1988-89....24
27. Salinities for scenarios 1, 3, 5, 7, and 9 near mouth of Townsend Bayou, 1988-89....24
28. Depths for scenarios 1, 4, 6, 8, and 10 near mouth of Goff Bayou, 1988-89....25
29. Salinities for scenarios 1, 4, 6, 8, and 10 near mouth of Goff Bayou, 1988-89....25

30. Full domain extent for EDYS Model for San Antonio Bay....26
31. Spatial extent of small EDYS models with black lines as approximate boundaries between small models....27
32. Vegetative responses for scenario 2....29
33. Vegetative responses for scenario 3....31
34. Vegetative responses for scenario 4....33
35. Average vegetative response south of the release point in Townsend Bayou during drought years for scenarios 5, 7, and 9 for drought years 1988-1989, 1995-1996, 2000-2001, 2008-2009, and 2011-2013....34
36. Average vegetative response of salt marshes lining Mission Lake during drought years for scenarios 6, 8, and 10 for drought years 1988-1989, 1995-1996, 2000-2001, 2008-2009, and 2011-2013....34
37. Vegetative responses to drought in 1995-1996 showing average extent for salt marshes lining Mission Lake by year (top) compared to flows in the Guadalupe River and timing of releases in Goff Bayou (bottom)....36
38. Vegetative responses to drought in 2000-2001 showing average extent for salt marshes lining Mission Lake by year (top) compared to and flows in the Guadalupe River and timing of releases in Goff Bayou (bottom)....37
B-1. Total aboveground biomass response for salt marsh, 0 percent woody community for scenarios 6, 8, and 10 (top) and location of this plant community (bottom)....44
B-2. Total aboveground biomass response for salt marsh, 5 percent woody community for scenarios 6, 8, and 10 (top) and location of this plant community (bottom)....45
B-3. Total aboveground biomass response for salt marsh, 18 percent woody community for scenarios 6, 8, and 10 (top) and location of this plant community (bottom)....46
B-4. Total aboveground biomass response for salt marsh, 0 percent woody community for scenarios 6, 8, and 10 (top) and location of this plant community (bottom)....47
B-5. Total aboveground biomass response for salt marsh, 5 percent woody community for scenarios 6, 8, and 10 (top) and location of this plant community (bottom)....48
B-6. Total aboveground biomass response for salt marsh, 18 percent woody community for scenarios 6, 8, and 10 (top) and location of this plant community (bottom)....49
B-7. Total aboveground biomass response for salt marsh, 0 percent woody community for inland saltgrass, marshhay cordgrass, Olney bulrush, and smooth cordgrass for scenarios 6 (green), 8 (red), and 10 (black), location of this plant community is shown Figure B-1....50
B-8. Total aboveground biomass response for salty prairie, 0 percent woody community for scenarios 5, 7, and 9 (top) and location of this plant community (bottom)....51
B-9. Total aboveground biomass response for salty prairie, 5 percent woody community for scenarios 5, 7, and 9 (top) and location of this plant community (bottom)....52
B-10. Total aboveground biomass response for salty prairie, 0 percent woody community for inland saltgrass and marshhay cordgrass for scenarios 5 (black), 7 (red), and 9 (green), location of this plant community is shown Figure B-8....53

B-11. Total aboveground biomass response for salty prairie, 5 percent woody community for inland saltgrass and marshhay cordgrass for scenarios 5 (black), 7 (red), and 9 (green), location of this plant community is shown Figure B-9.....54
B-12. Total aboveground biomass response for common reed in salt marsh communities on Mission Lake for scenarios 6 (green), 8 (red), and 10 (black), locations of these plant communities are shown Figures B-1 through B-3 55

Abstract

The San Antonio River Authority has responsibilities for both water quality and quantity management in the San Antonio River and its tributaries. The San Antonio River flows into the Guadalupe River just upstream of the bay and estuary system that includes San Antonio Bay. The complexities of the linked river and bay ecosystems make simple single-factor management approaches inadequate for effective management. Since 2011, the research team has used the EDYS model to simulate water and vegetation conditions for the watersheds along the river and around San Antonio Bay. In this project, the research team used the TELEMAC-2D hydrodynamic model to assemble a two-dimensional water and salinity circulation model. Using available data to represent river inflows, tidal water levels, salinity, and wind variations for 1987-2013, the TELEMAC-2D model successfully simulated variations in water level, velocities, and salinity across the bay and estuary system, with runoff from the watershed surrounding San Antonio Bay provided by the EDYS model. The hydrodynamic model provided simulated water levels and salinities at the coastal edges and marshes of San Antonio Bay for input to the EDYS model's simulation of spatial and temporal vegetation dynamics. Ten scenarios were investigated, including baseline conditions and nine different diversions or additions of freshwater to selected inflow locations at selected times. The EDYS outputs demonstrated the importance of flow intensity and timing on marsh vegetation, as well as potential trade-offs between various parts of the bay system. These tools are ready for additional applications.

Acknowledgements

The authors gratefully recognize Terry McLendon for his important role in all of the EDYS-related work for the San Antonio River Authority over many years, both as part of the Texas Tech University team and with KS2 Ecological Services. His critical insights and advice were necessary to best interpret our modeling results. J.D. Booker, Cindy Dickson, and Leo Richarte also contributed to the data collection and modeling efforts as part of the long-time EDYS team. We thank Steve Raabe, Shaun Donovan, and Melissa Bryant of the San Antonio River Authority for their active partnership in this project. Useful comments were also received from Nathan Pence and Thomas Hill of the Guadalupe-Blanco River Authority, Myron Hess of Myron Hess PLLC, Kyle Garmany of the Nature Conservancy, and Paul Montagna of the Harte Research Institute for Gulf of Mexico Studies at Texas A&M University-Corpus Christi. Sam Vaugh and Zach Stein of HDR, Inc., provided freshwater inflow data for the simulation period based on their previous water availability modeling experience.

1 Introduction

San Antonio Bay is one of the six major bays on the Texas Gulf Coast. The San Antonio River flows into the Guadalupe River approximately 12 miles northwest of the mouth of the Guadalupe, from which the combined flows enter San Antonio Bay. The San Antonio River Authority has the dual responsibilities of managing water quality and quantity in the San Antonio River and its tributaries. The relative proportions of freshwater and saltwater and the quality of the freshwater entering the Bay are important to the River Authority, because decisions made by the River Authority affect both the quality and quantity of this major freshwater supply to the San Antonio Bay.

The River Authority recognizes the importance of making good management decisions relative to both the San Antonio River and San Antonio Bay ecosystems. However, both ecological systems are complex, such that simple single-factor approaches are often inadequate to provide the necessary tools for effective management of these linked systems. One substantially beneficial tool for decision makers in the San Antonio River-San Antonio Bay complex is a dynamic ecological simulation model that can integrate hydrological and ecological responses in a practical and scientifically valid manner.

EDYS is a dynamic ecological simulation model that is mechanistically based and spatially explicit. It has been widely used for ecological simulations, watershed management, land management decision making, environmental planning, regulatory compliance, and revegetation and restoration design analysis, with projects in Texas, 11 other states, and international sites. Previous EDYS county-wide models have been built for applications for the River Authority and the Texas State Soil and Water Conservation Board for counties along the river from San Antonio to the Gulf Coast (McLendon et al. 2012, 2015, 2016, 2018).

The River Authority is interested in the potential of EDYS to provide an integrated management tool for use on the San Antonio River watershed, including San Antonio Bay. Tasks to develop the simulation tools for use on the watershed and the bay have been ongoing since 2011, first with KS2 Ecological Field Services and then with Texas Tech University (TTU). One of the desired uses of this integrated management tool is the ability to evaluate the impacts of differing freshwater inflows arriving via the Guadalupe River on the marsh vegetation along the bay. Phase 6 included the development of an extended footprint model for the bay, and the River Authority has expressed interest in using this extended model for evaluating different freshwater inflows on marsh vegetation. Proper representation of the water and salinity circulation in San Antonio required application of a two-dimensional hydrodynamic model to the shallow estuary conditions, including the emphases on wind and tidal variations that also drive the circulation processes. The TELEMAC-2D hydrodynamic model successfully met this challenge, and the research team developed a sequential process to couple TELEMAC-2D and EDYS to satisfy the River Authority's needs. This report documents the assembly of the

hydrodynamic model for the estuarine system, procedural linkage to the EDYS model of the local watersheds, and simulation of ten predictive "what-if" scenarios to demonstrate the abilities of the model tools to describe the ecosystem responses.

2 TELEMAC-2D Model

TELEMAC-2D is the main code of the computational fluid dynamics (CFD) software suite, TELEMAC, which was developed to solve the two-dimensional depth-averaged free surface flow Saint-Venant equations (Ata 2020, Mattic 2020a, b). Two assumptions made to derive the Saint-Venant equations from the general comprehensive three-dimensional Navier-Stokes equations: (1) water depth is small compared with the horizontal flow length scale, and (2) no density stratification exists in the simulation domain. The second assumption implies that variable and parameter changes in the vertical direction are negligible, and the vertical averages presents the correct estimates of these components. With this simplification, TELEMAC-2D can simulate complex systems such as tidal waves, floods, and tracer movement in shallow water.

Different CFD phenomena have different requirements, such as complex boundary conditions, nonuniform initial conditions, and linkages with a secondary program. TELEMAC-2D provides a set of FORTRAN subroutines designed to observe these requirements. This consideration helps the users to be able to use this model in many applications including effects of dam failures, hydraulic structures (bridges, culverts, and levees), and water and salinity circulation in estuaries. TELEMAC-2D uses the finite element method (FEM) to discretize the Saint-Venant equation through triangular grids in the two-dimensional space and consider vertically averaged variables like velocities and tracer solute concentrations. The main advantage of the FEM over the finite difference method (FDM), another common numerical solution method, is storing the information in elements rather than nodes. This technique helps the discretized mesh to adapt to irregular solution domains, as the triangular elements can be generated with different lengths and angles.

2.1 San Antonio Bay Application

In this study, the TELEMAC-2D model was used to simulate the water and salinity patterns in San Antonio Bay and nearby estuarine water bodies based on two major assumptions. For simplicity, this bay circulation model is referred to as the SA Bay model in this report. First, San Antonio Bay was considered to be a shallow estuary with average depth of about 1 meter (3 ft) over the entire domain. The shallow water circulation produced by inflow, tides, and winds causes sufficient vertical mixing throughout the bay to keep vertical changes in salinity small enough that the average value throughout the depth is a good approximation. Second, the density of water is also assumed constant in all directions in the computational domain. This assumption is applicable vertically, as the water is effectively mixed across the shallow depth. The density of water may vary temporally and spatially caused by changes in salinity. Spatial variation in water density was not included to avoid adding more complexity to the model. The model spatial domain is shown in Figure 1, with approximate subdivisions for various named water bodies.

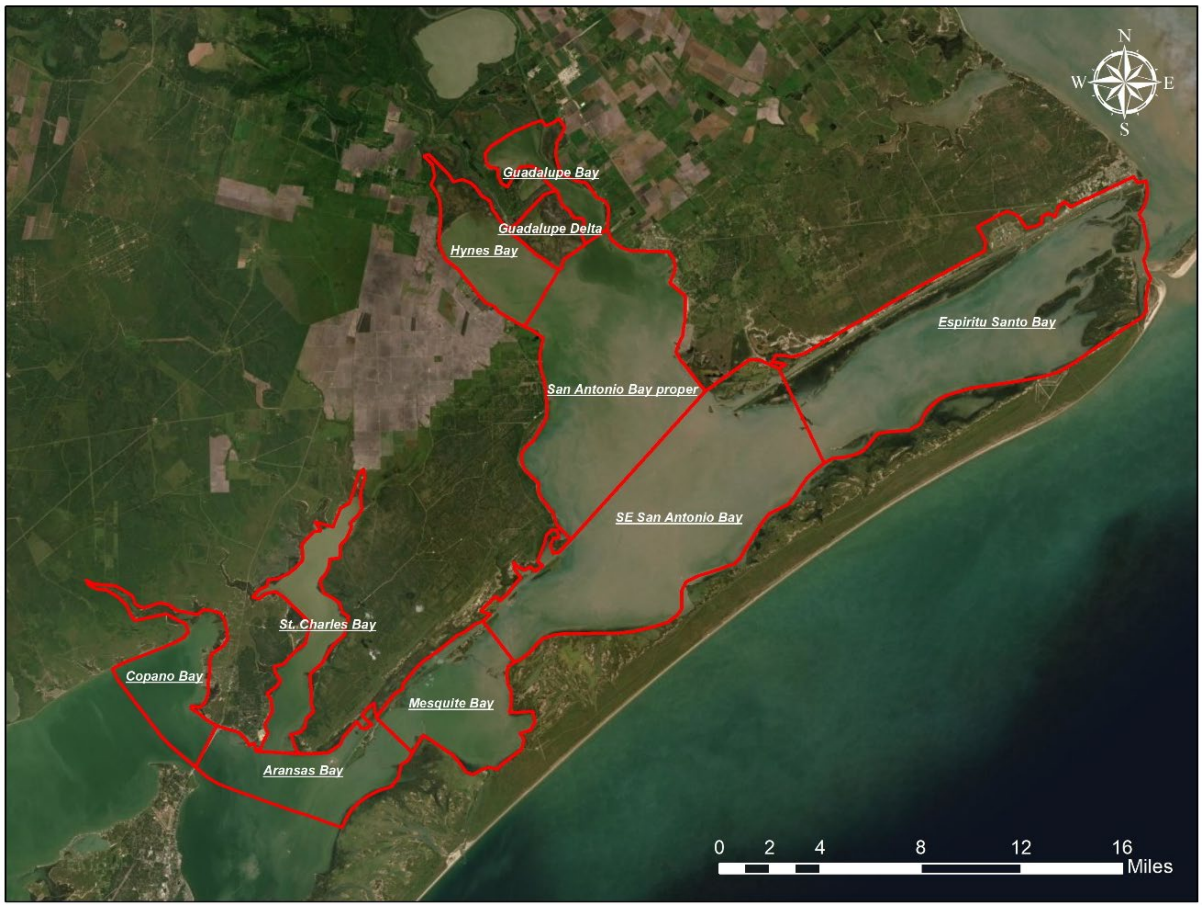

Figure 1. General location of the solution domain for the SA Bay model

2.2 Data Requirements

The bathymetry dataset associated with this study was 40-m raster data collected and provided by the River Authority staff. The data extended from Mission Lake, Guadalupe Bay, and Hynes Bay to the north, San Antonio Bay at the center, Mesquite Bay, St. Charles Bay, and parts of Aransas Bay and Copano Bay to the west, and Espiritu Santo Bay to the east. The small islands on the eastern side of Espiritu Santo Bay form the barrier at the mouth of the bay to the Gulf of Mexico and protect the bay from waves with high amplitudes. However, this barrier creates a restriction for water to move freely between two places. The only connections between the ocean and the Espiritu Santo Bay are the narrow straits named Big Bayou and Saluria Bayou. Our simulations predated the new connection to the ocean constructed at the south end of Matagorda Island. To make sure that the connection between the ocean and bay was represented in the model's domain, the bathymetry grid was adjusted by widening the straits. This change also helped to reduce the instability caused by wave reflection near the boundary. The total area of the solution domain was 772.16 km^2 (299.51 mi^2). Elevations of the estuary bottom ranged from 0 to 11.73 m below mean sea level, and the total volume below mean sea level was 744.28 km^3 (178.43 mi^3, 6.029×10^8 ac-ft). The resulting average depth of the bottom below mean sea level was 0.984 m (3.23 ft) with standard deviation of 0.741 m (2.43 ft).

2.2.1 Model Domain

The solution domain for the TELEMAC-2D SA Bay model was discretized into an irregular triangular mesh to facilitate application of the FEM and ensure model stability. Three main factors influenced the size and shape of the model mesh: (1) Courant number (CN), (2) run time, and (3) computation file sizes. In a two-dimensional system,

$$CN = \frac{u_x \Delta t}{\Delta x} + \frac{u_y \Delta t}{\Delta y} \quad (1)$$

where Δt = time step, Δx and Δy are element dimensions in the x and y directions, respectively, and u_x and u_y are components of the local velocity vector in the x and y directions, respectively. CN shows how fast water and salinity information is passing through the elements. Numerical stability is more likely when the CN is less than one, ensuring that water and salinity can only travel from one element to an adjacent element during each time step. TELEMAC-2D does include the ability to stabilize the model with CN greater than one, but preference is for CN less than or equal to 1. Choosing the mesh size for small CN corresponds to small time steps, which tend to increase run time and computation file size. In the final mesh, the distances between triangular element nodes vary between 200 m near the freshwater inflows and 1000 m in the deeper middle of the bay. A time step of 5 mins or 300 sec was sufficient to keep the maximum CN no larger than 1.0. As a result, 1644 nodes and 2689 elements were allocated to represent the water movement and salinity distribution in the SA Bay model domain. Figure 2 shows the mesh relative to the metric UTM coordinates as rendered by the Blue Kenue utility software that allows visualization of the TELEMAC-2D input and output data. The subdivisions of the SA Bay model from Figure 2 were inserted for perspective.

2.2.2 Boundary Conditions

Three types of boundary conditions were considered for this model. First, the open boundaries at the eastern and western ends of the SA Bay model had to communicate the tidal variations provided by the TxBLEND simulations, shown as green nodes in Figure 3. The Thompson method was selected in TELEMAC-2D to allow specification of the water surface elevations at the green nodes to drive calculation of corresponding velocities and flow rates at these boundaries. The Thompson method uses the method of characteristics to describe the outgoing and incoming waves at non-reflecting boundary conditions (Thompson 1987). Second, the coastlines of Matagorda and San Jose islands of the SA Bay model were set as no-flow boundaries. Blue nodes in Figure 3 designate those locations. Third, the remaining nodes were set as prescribed flow to accommodate the river or bayou inflows (red nodes in Figure 3) from historical data or runoff inflow (gold nodes) from the EDYS simulations. Detailed data for the river/bayou channel cross-sections and local runoff channels were not available, so these inflows were communicated to TELEMAC-2D as volume additions to the continuity equation rather than momentum additions using a net precipitation rate applied over the effective area near the inflow node.

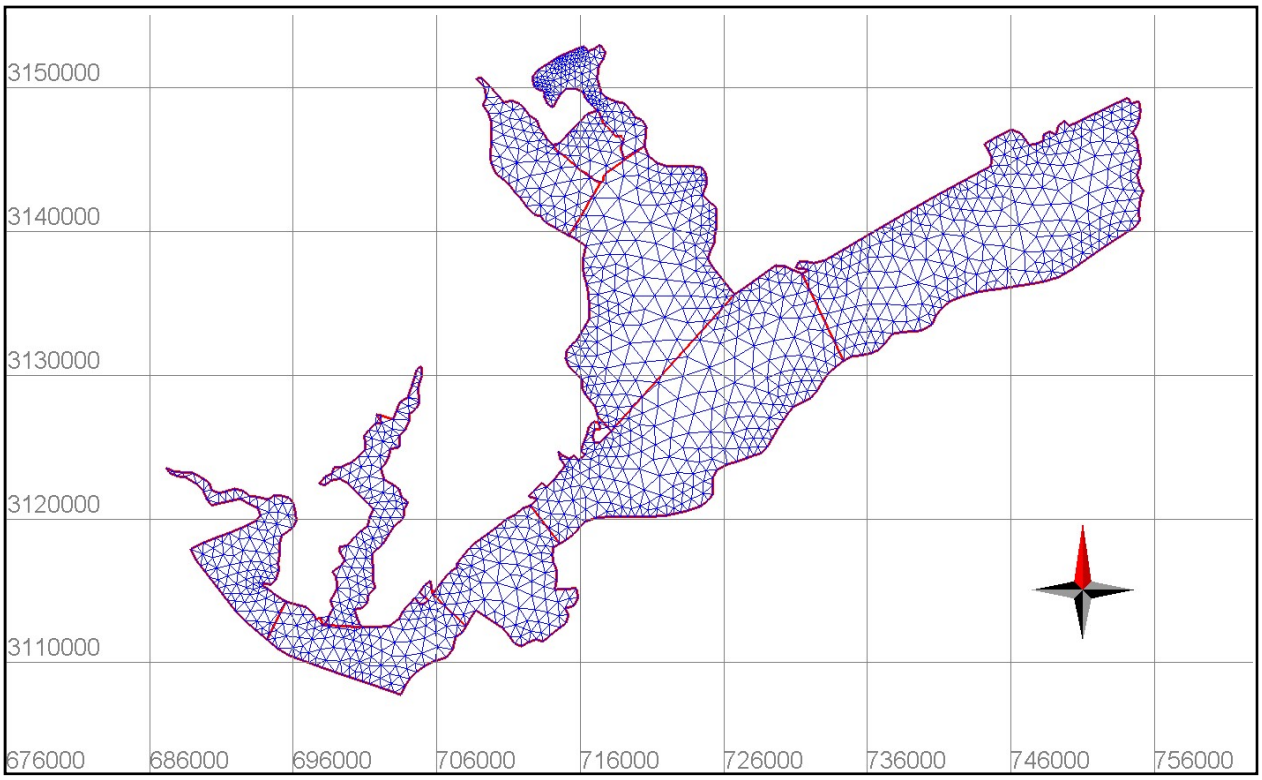

Figure 2. Finite element mesh with 1664 nodes and 2689 triangular elements

2.2.3 Hydrologic Variables

The simulation period chosen for this study was 27 years based on historical data available for the calendar years 1987 through 2013, as used by HDR, Inc., engineers in their water availability modeling for the San Antonio and Guadalupe rivers. The model runs started at midnight on the first day of January 1987 and ended on December 31, 2013 at midnight. The time step of the simulation was fixed to 5 mins to ensure numerical stability. Linear interpolation was used to convert input variables provided at other time intervals to 5-min values.

Variations in salinity and water surface water elevation relative to mean sea level represented the tidal impacts at the open southwest and northeast boundaries of the model domain. The modeling staff of the Texas Water Development Board (TWDB) generated a dataset for our simulation time period with their TxBLEND model of the Guadalupe and Mission-Aransas estuaries (Guthrie 2010), which includes our SA Bay model. TxBlend simulation results provided hourly values of water surface elevation and salinity for its corresponding grid locations nearest to the TELEMAC-2D tidal boundary nodes. Those values were interpolated for specification at those boundary nodes.

Wind data were critical to proper simulation of circulation of the water and salinity in northern and central portions of the SA Bay model. The most complete wind dataset was available from the National Climatic Data Center for the station known as Rockport Aransas

Figure 3. TELEMAC-2D initial boundary nodes, with 27 freshwater inflow nodes (red), 50 TxBLEND tidal nodes (green), 491 runoff nodes (gold), and 520 no-flow nodes (blue)

County Airport, Texas, GHCND:USW00012972, latitude 28.08361°, longitude -97.04639° (Robel 2019). The hourly data included wind speed and direction. Figure 4 shows the location of the weather station relative to our SA Bay model.

TELEMAC-2D required net precipitation input values. Net precipitation describes the total amount of rainfall that remains after subtracting evaporation from gross rainfall. These values were most often negative as appropriate for dates without rainfall. Daily precipitation data were taken from the weather station at Austwell, Texas, GHCND:USC00410436, latitude 28.389º, longitude -96.8388º, on the west side of Hynes Bay. Monthly evaporation data came from the TWDB (2019) website for quadrangle 911 that includes the study area. The daily and monthly values were assumed to be uniform over those time intervals, then converted to the required TELEMAC-2D time step.

Freshwater discharges were described by data used by HDR, Inc., in their water availability modeling work for the River Authority and other clients. The flows came from the Guadalupe and San Antonio rivers and were then directed through five channels, Goff Bayou, Hog Bayou, Schwings Bayou, Guadalupe River at Traylor's Cut, and Guadalupe River below

Figure 4. Location of Aransas County Airport relative to SA Bay model

Traylor's Cut, into Mission Lake. Daily values for each of the five channels were provided to TELEMAC-2D at the red nodes in Figure 3. The other source of freshwater was daily runoff generated by the EDYS model and introduced at the gold nodes in Figure 3. It should be noted that freshwater inputs could be changed at selected locations for different predictive scenarios.

2.2.4 Quality Data

Movement of salinity was simulated as a conservative tracer in TELEMAC-2D. Salinity concentrations in ppt were provided as hourly time series data selected from the output nodes of the TxBLEND model adjacent to the open boundary lines, noted as the green nodes in Figure 3. The freshwater sources included the five channels in the north part of the bay, precipitation, EDYS runoff, and diversions or additions in the predictive scenarios. The salinity concentration for all freshwater sources was assigned a constant value of 0.1 ppt to avoid problems in the model calculation process.

2.3 TELEMAC-2D Model Settings

2.3.1 Physical Parameters

TELEMAC-2D required two additional physical parameters that are specific to each application depending on its geometry and the physical flow phenomena. These two parameters described the friction force and turbulence conditions in our SA Bay model. First, the effect of friction force was represented by Manning's equation, and the Manning roughness was set at 0.020 for the entire domain. Although the variation in friction coefficient can alter the depth and velocity locally due to energy loss, the assumption is reasonable based on the range of depth changes and the purpose of this study. Second, the effects of turbulent mixing and eddy dissipation can be captured with four different approaches in TELEMAC-2D: constant viscosity coefficient, Elder model, *k*-ε model, and Smagorinski model. The TELEMAC-2D documents indicated that the estuary conditions in this model were best simulated with the constant viscosity coefficient method with a velocity diffusivity of 0.01. Based on the small typical velocities (~ 1 m/sec) and large mesh size (200 to 1000 m), the choice of velocity diffusivity had no impact on the numerical solutions.

2.3.2 Numerical Scheme

TELEMAC-2D, like other numerical systems, uses different numerical schemes to provide more flexibility in solving the partial differential equations based on the problem of interest. Considering the conservative form of the Saint-Venant finite element equations, the wave equation approach was selected to treat this linear system, considering that depth and velocities changed linearly in space. This consideration helps to keep the simulation model fast, while smoothing the results by eliminating the momentum advection (Mattic 2020).

The other notable consideration made in the scheme is treatment of dry zones known as tidal flats. To distinguish between dry and wet elements in the FEM, TELEMAC-2D uses three different techniques: (1) free surface gradient correction, (2) masking the tidal flats, (3) and adding a porosity term to tidal flat areas (Mattic 2020). In this study, the first technique was applied along with flux limitation conditions to preserve the conservation of mass and to abandon negative depths at the wet and dry element thresholds.

To solve the partial differential equations by the FEM, the TELEMAC-2D model uses the fractional steps method when the method of characteristics is activated. This method separates the advection from the propagation and diffusion terms of the equation and computes the intermediate values for the advection stage, then uses the intermediate values to solve the rest of the equation separately in the other step (Hervouet 2007). Different distribution schemes can be applied to find the optimal values for the intermediate term. To get sharp convergence, the N distribution scheme, including the non-linear positive streamwise invariant (PSI), was used to solve the advection stage of the depth in the fractional step method.

2.3.3 Tracer Calculations

The transport or tracer equation, like the mathematical tidal hydrodynamic equations, was applied through the domain by averaging parameters and variables over the vertical depth. This equation was solved sequentially with the tidal flow equations through each time step. To begin the solution process, the initial guess value of for salinity concentration was 35 ppt for the entire domain, and the model found its converged equilibrium condition for each time step through the simulation process. Based on sensitivity tests, the diffusion coefficient of the solute obtained to be equal to 0.01 (based on the maximum mesh size). The diffusion coefficient is strongly dependent on the mesh resolution, even if it is difficult to differentiate its impact. However, evaluating the spatio-temporal effect of the diffusion coefficient on the tracer concentration was beyond the scope of this research, and that topic was left for future studies. To solve the advection part of the equation, the edge-by-edge implication of the N-Distributive scheme solution was chosen to preserve the conservation of the tracer. Finally, the minimum error form of the conjugate gradient method was selected as the solver for the transport equation.

2.4 TELEMAC-2D Preliminary Applications

As stated previously, the time period of interest for the TELEMAC-2D simulations was calendar years 1987 through 2013 based on the dataset of river and bayou inflows provided by HDR, Inc., as used in related water available modeling efforts for the River Authority and others. With 5-min time steps in the 27-yr simulations, the typical computer run time was about 9 hrs on a 64-bit desktop with a i7-6700 3.40 GHz CPU with 16 GB of RAM. Each simulation provided large output files for the spatial distributions of water depths, velocity vectors, and salinities across the nodes in the SA Bay model. The Blue Kenue pre- and post-processor allowed visualization of the spatial distributions as single time snapshots or as animations. While the animations are most representative of TELEMAC-2D's capacity to simulate the temporal changes in all three variable types, this report document allows only selected snapshots. Interested readers may contact the authors for access to presentations with selected animations. Figure 5 provides the simulated distribution of water depth across the SA Bay model at 12:00 a.m. on July 29, 2005. Water depth changes over time ranged from 0 to over 1 m depending on node locations. Figure 6 displays the simulated salinity distribution for 12:00 a.m. on July 29, 2005. The water body subdivisions were added for clarity. This figure indicates the influence of the freshwater inputs at the northern end of Guadalupe Bay, as well as the high salinity tidal input at the eastern end of Espiritu Santo Bay. Snapshots of velocity vectors were less impressive, but animations clearly demonstrated changes in flow directions caused by the temporal variations in freshwater and tidal flows.

Salinity observations were available at three locations in the SA Bay model as shown in Figure 7, one near the Aransas National Wildlife Refuge (ANWR), the second in Mesquite Bay,

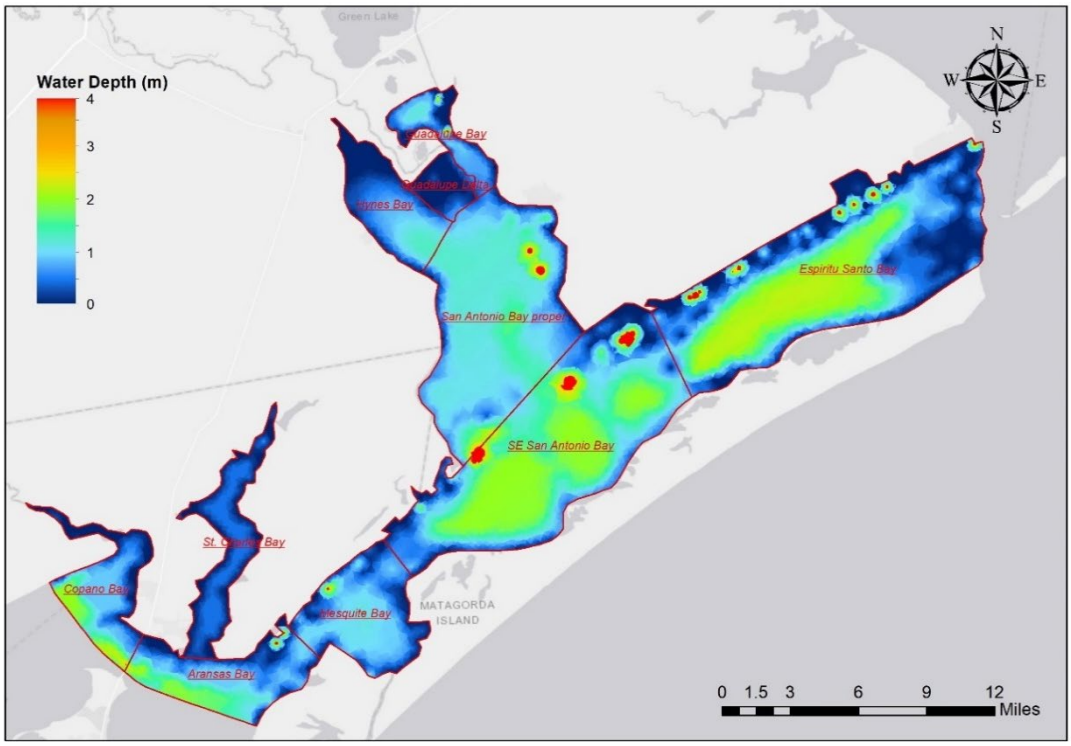

Figure 5. Simulated depth distribution for 12:00 a.m. July 29, 2005

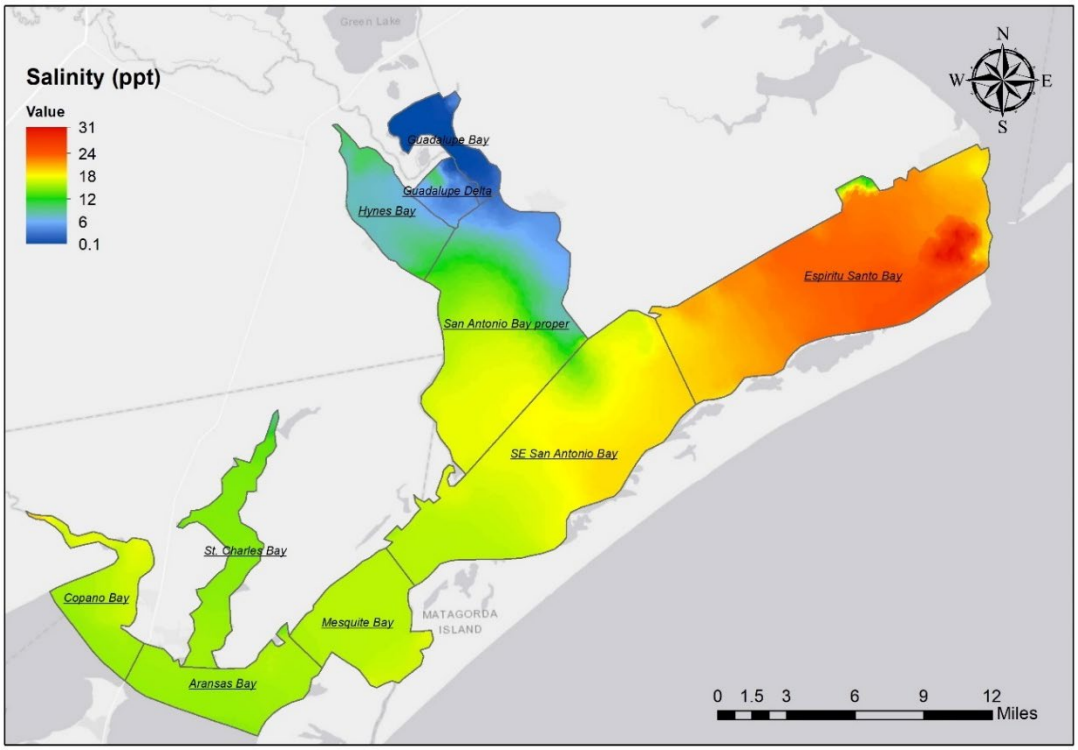

Figure 6. Simulated salinity distribution for 12:00 a.m. July 29, 2005

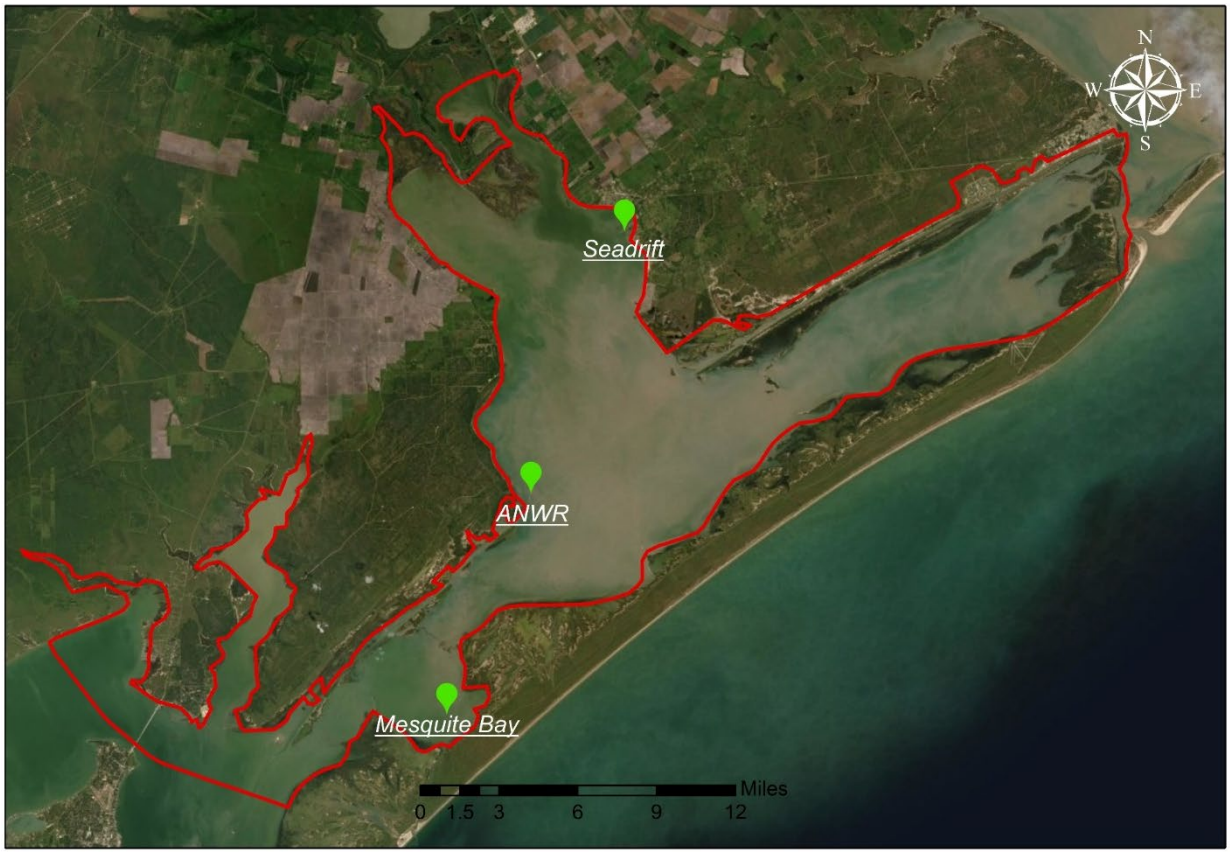

Figure 7. Locations of salinity observations

Table 1. Salinity Observation Stations

Data Descriptor	ANWR	Mesquite Bay	Seadrift
Start date and time	2/23/2004 22:00	1/1/2009 0:00	1/1/2012 0:00
End date and time	12/31/2013 23:00	12/31/2015 23:00	12/31/2015 0:00
Number of records	77175	51703	25644
Number missing	9203	9641	9420
Maximum salinity (ppt)	50.1	44.2	32.1
Minimum salinity (ppt)	0	3.3	0

and the third near Seadrift. The respective periods of record are shown in Table 1, and the simulation ended on December 31, 2013. These data were taken at face value, and missing data values were left as blanks. It is also worth noting that the observation locations did not directly align with nodes in our mesh. Figures 8 to 10 show that the distances between the observation sites and the nearest model nodes ranged from 250 m to 306 m.

Figures 11 to 13 compare the TELEMAC-2D simulated salinity values with the observations at the three respective sites. In all three figures, the black lines represent the observed salinity data, the red lines indicate the simulated salinities based on freshwater flows

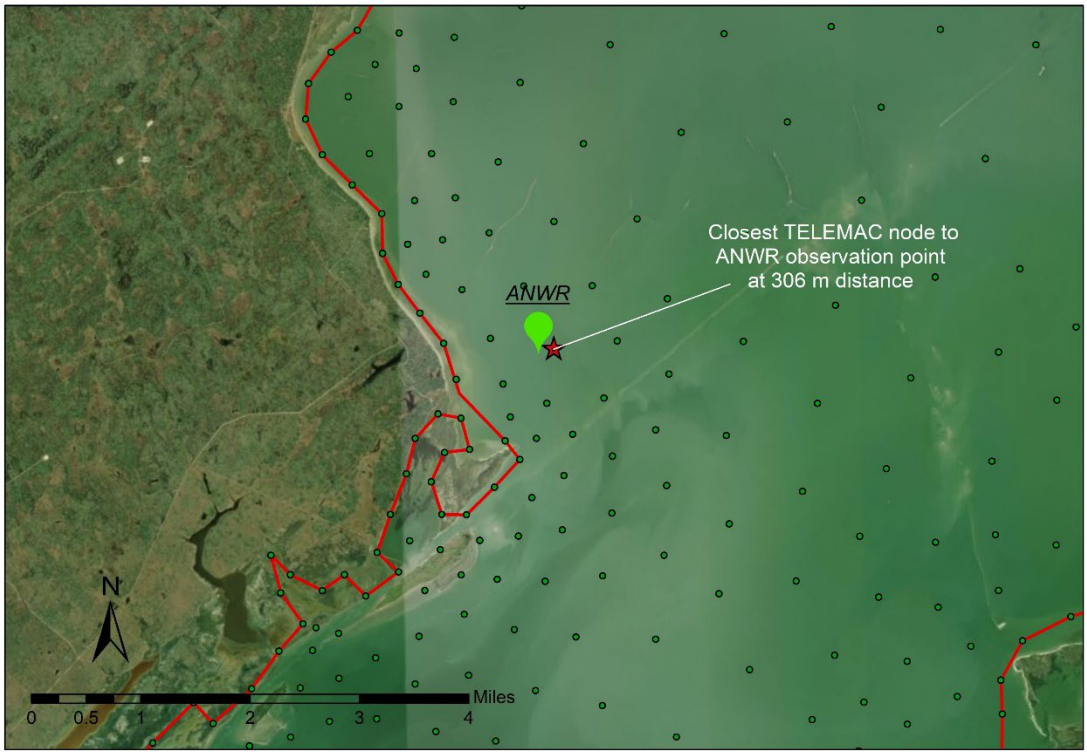

Figure 8. Comparison of nearest model node location to ANWR monitoring site

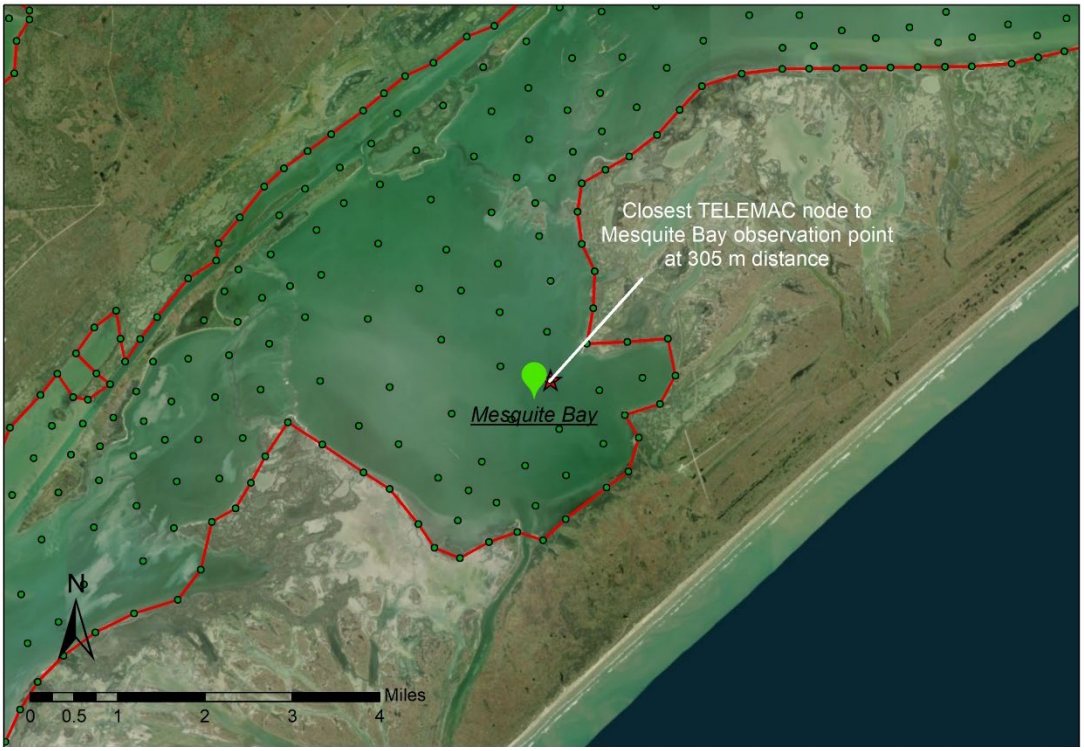

Figure 9. Comparison of nearest model node location to Mesquite Bay monitoring site

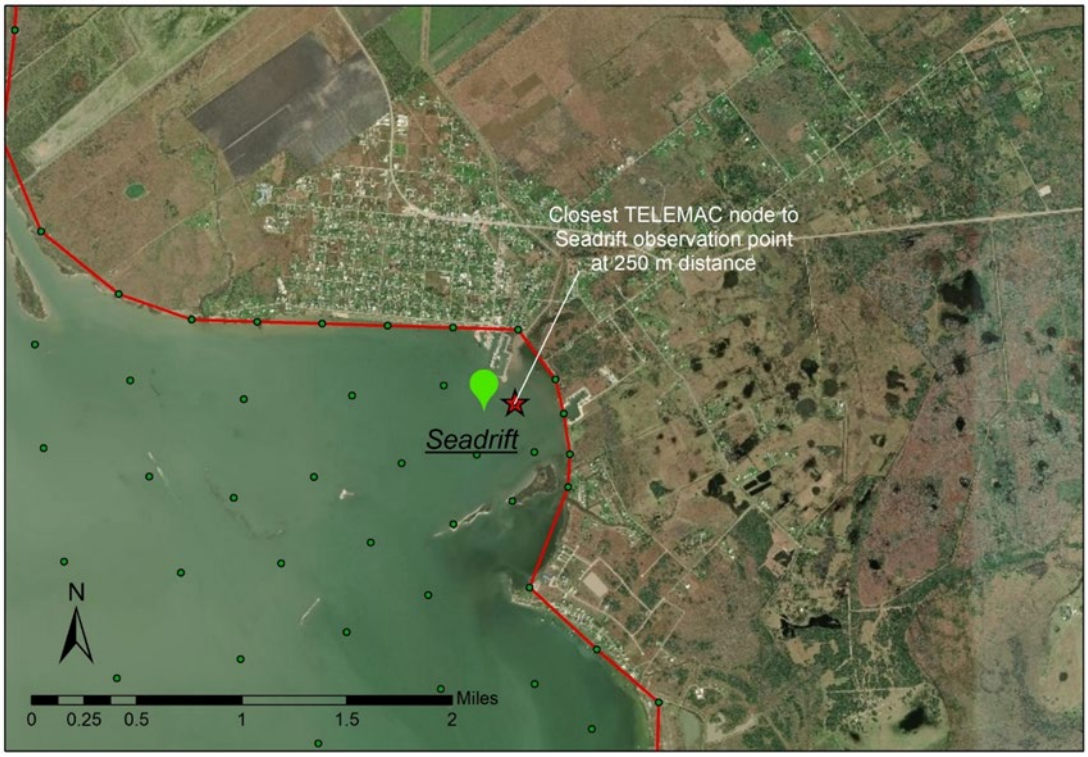

Figure 10. Comparison of nearest model node location to Seadrift monitoring site

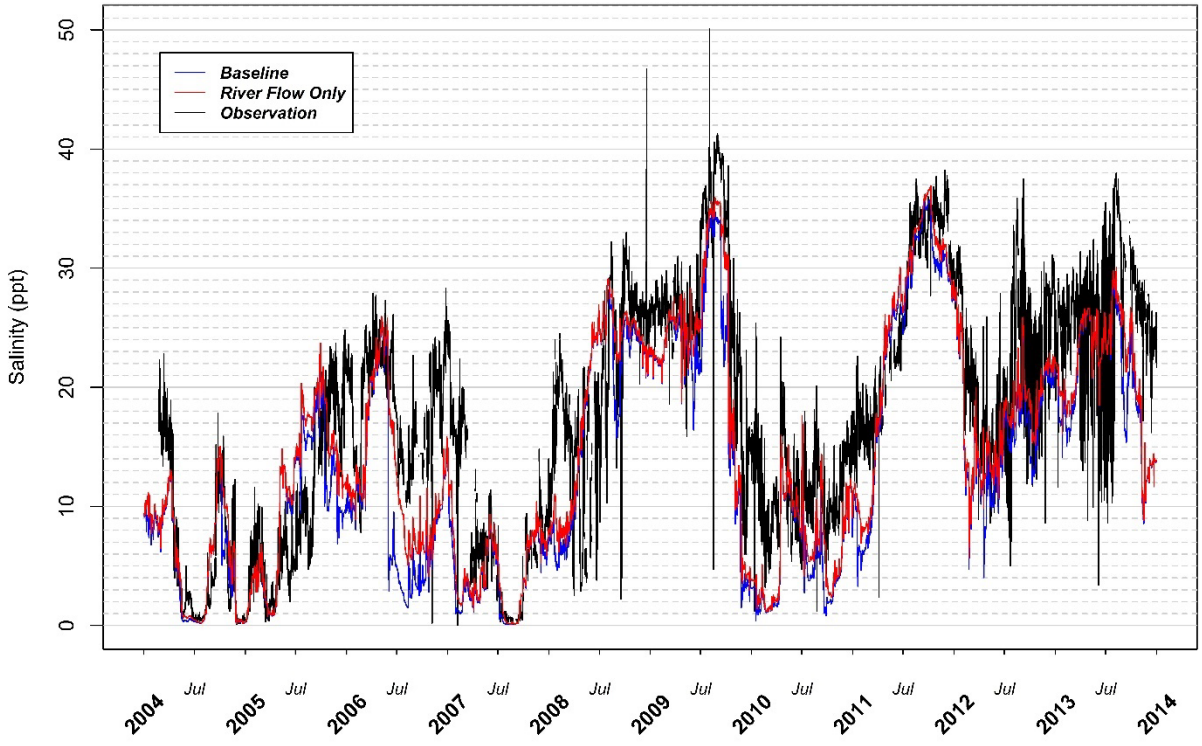

Figure 11. TELEMAC-2D simulation and observed data at ANWR monitoring site

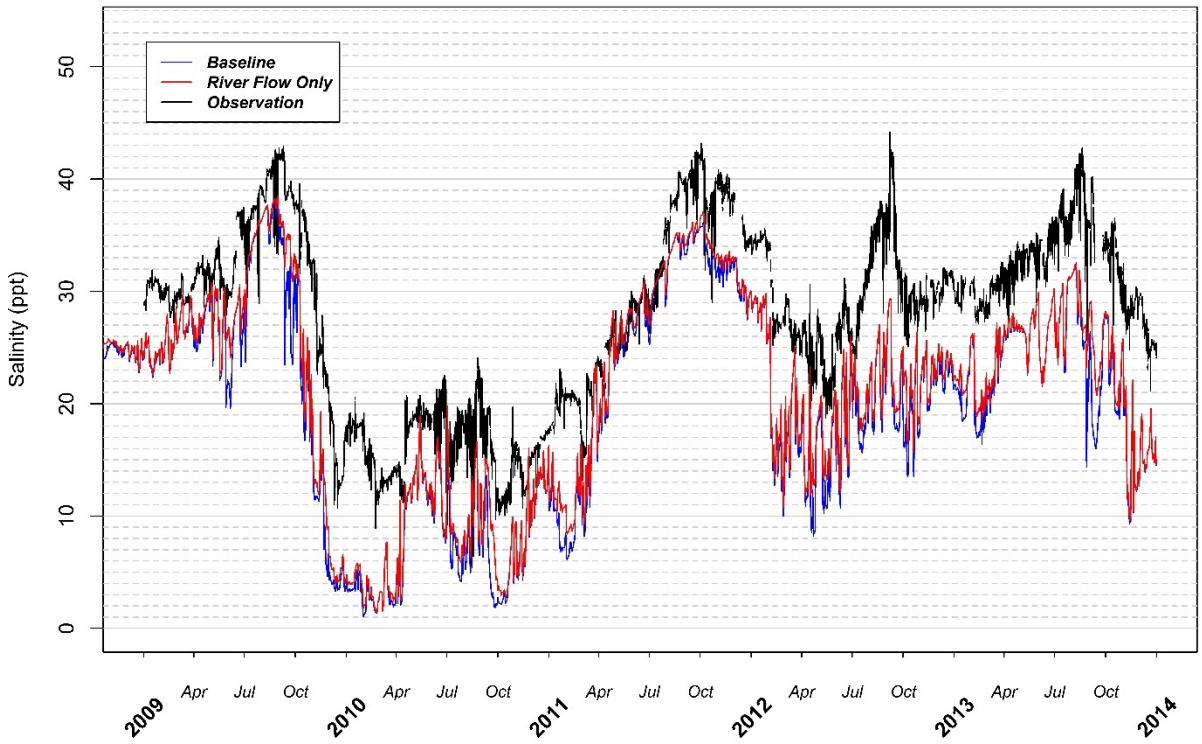

Figure 12. TELEMAC-2D simulation and observed data at Mesquite Bay monitoring site

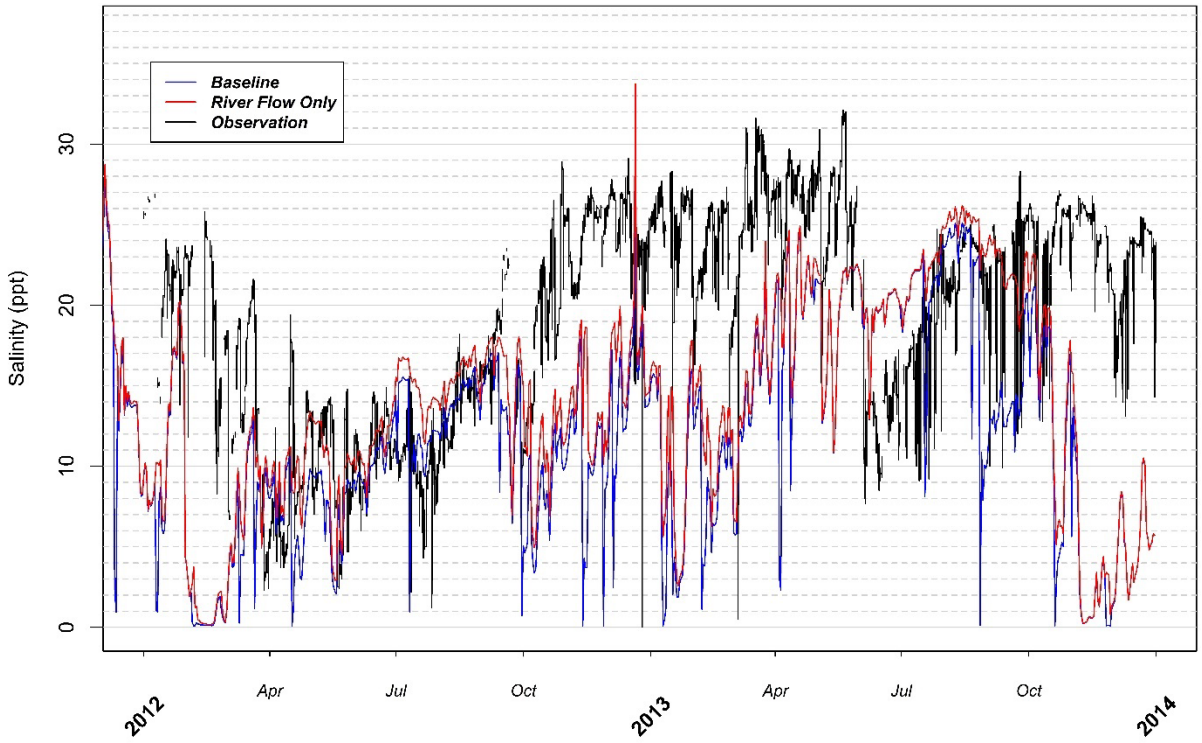

Figure 13. TELEMAC-2D simulation and observed data at Seadrift monitoring site

from the river and bayou inflow dataset, and the red lines resulted from simulation of freshwater flows from the river and bayou dataset plus simulated runoff from the EDYS model for the San Antonio Bay vicinity, which will be discussed in a subsequent section. The added freshwater runoff consistently lowered the simulated salinity values, but the amount of decrease varied as the runoff and freshwater flows varied. The combination of the runoff with the river and bayou flows was referred to as the baseline scenario. The longest record at almost 10 years for comparison was at the ANWR location. As seen on Figure 11, the large-scale seasonal variations were simulated well for most of the time period, with the observed data higher than simulated about 20 percent of the time. In Figure 12, the simulated and observed seasonal trends at the Mesquite Bay location were similar across the five years, but the observed salinity values were offset 5 to 10 ppt above the simulated values. The pertinent observation time was two years at the Seadrift location, and this record had the largest fraction of missing data. Figure 13 shows the simulated and observed salinities were most similar in March to October of 2012 and August to October of 2013, but the simulated salinities were often much lower than the observations in the other months.

It should be noted that all of the river and bayou inflow values as well as the tidal boundary water levels were estimates provided by others, and it is possible that those estimates may have been sometimes unrealistic. The single wind data location at the Aransas County airport is just outside the SA Bay model domain, at distances of about 33 km (20 mi), 28 km (17 mi), and 49 km (30 mi) from the ANWR, Mesquite Bay, and Seadrift salinity observation stations. It is likely that wind speeds and directions varied over these distances, which could greatly affect the TELEMAC-2D simulation. The salinity observations were taken at face value for comparison to the simulated results. Still, these limited flow, wind, and salinity data were the best available information for these serious efforts to simulate water and salinity circulation in this large estuary system. The TELEMAC-2D results demonstrated sufficient sensitivity to the variable inputs to be acceptable for coupling with the EDYS ecohydrological model for other predictive simulations. Future applications could pursue more sources of the pertinent input data.

3 Hydrodynamic Scenario Simulations

The research team and the River Authority staff cooperated in phases to develop ten freshwater inflow scenarios for simulation with the coupled TELEMAC-2D and EDYS models. Four initial scenarios were defined, simulated, and reviewed in the first phase. These four are shown in Table 2. The first scenario was the already completed baseline condition, using the HDR, Inc., water availability model river and bayou inflows plus the EDYS runoff along the north coastlines. Scenario 2 considered redirection of 10,000 ac-ft/yr (14 cfs, 8.9 MGD) spread out over the entire year from the Guadalupe River below Traylor's Cut to the Boat Canal on the Guadalupe Delta lobe (Delta). This redirection is shown on Figure 14. In scenario 3, 25,000 ac-ft/yr (35 cfs, 22 MGD) were taken from the Guadalupe River above the Guadalupe-Blanco River Authority (GBRA) Saltwater Barrier and moved to Townsend Bayou upstream of Hynes Bay, as

Table 2. Scenarios for Coupled TELEMAC-2D and EDYS Simulations

Scenario	Source	Amount (ac-ft/yr)	Diversion Location	Delivery Location
1	Natural	Baseline Historical Flows	N/A	N/A
2	Redirect	10,000	Guadalupe River below Traylor's Cut	Boat Canal on Guadalupe Delta Lobe
3	Redirect	25,000	Guadalupe River above GBRA Saltwater Barrier	Townsend Bayou - Hynes Bay
4	New	25,000	N/A	GBRA Canal System (Goff Bayou)
5	New	5,000 (June drought years)	N/A	Townsend Bayou - Hynes Bay
6	New	5,000 (June drought years)	N/A	GBRA Canal System (Goff Bayou)
7	New	5,000 (July drought years)	N/A	Townsend Bayou - Hynes Bay
8	New	5,000 (July drought years)	N/A	GBRA Canal System (Goff Bayou)
9	New	3,000 (July drought years)	N/A	Townsend Bayou - Hynes Bay
10	New	3,000 (July drought years)	N/A	GBRA Canal System (Goff Bayou)

shown in Figure 15. Scenario 4 introduced 25,000 ac-ft/yr of new water at Goff Bayou in the GBRA Canal System as shown in Figure 16. The results of these four scenarios were reviewed to determine appropriate freshwater flow conditions for the remaining scenarios.

The decision for the final phase was to explore targeted one-month flow additions in summer months of historical multiyear droughts during the 1987-2013 time period. The multiyear droughts were defined by relatively low flows from the Guadalupe River in the summer months. Analyses of the monthly data identified five multiyear droughts: 1988-89, 1995-96, 2000-01, 2008-09, and 2011-13. Figures 17-21 show the Guadalupe River monthly average flow rates for the time periods that include the five respective multiyear droughts. A frequency analysis of the 27 years of monthly flow values yielded 5 percent (375 cfs) and 10 percent (589 cfs) monthly non-exceedance probabilities (MNEPs) that are also shown on those figures to identify low flows. Considering the importance of flow during the growing season for some vegetation types, the new 5,000 ac-ft were applied in the month of June (84 cfs, 54 MGD) for the drought years at either Townsend Bayou or Goff Bayou for scenarios 5 and 6,

Figure 14. Scenario 2 diversion

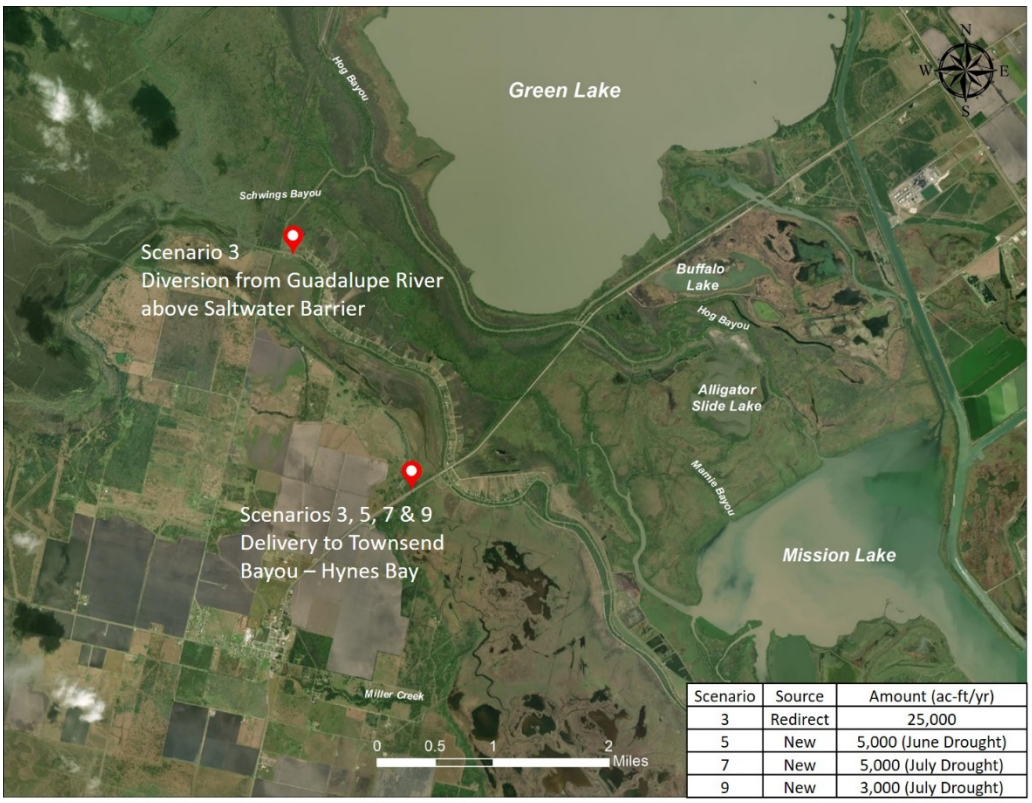

Scenario	Source	Amount (ac-ft/yr)
3	Redirect	25,000
5	New	5,000 (June Drought)
7	New	5,000 (July Drought)
9	New	3,000 (July Drought)

Figure 15. Scenario 3 diversion and scenarios 5, 7, and 9 additions

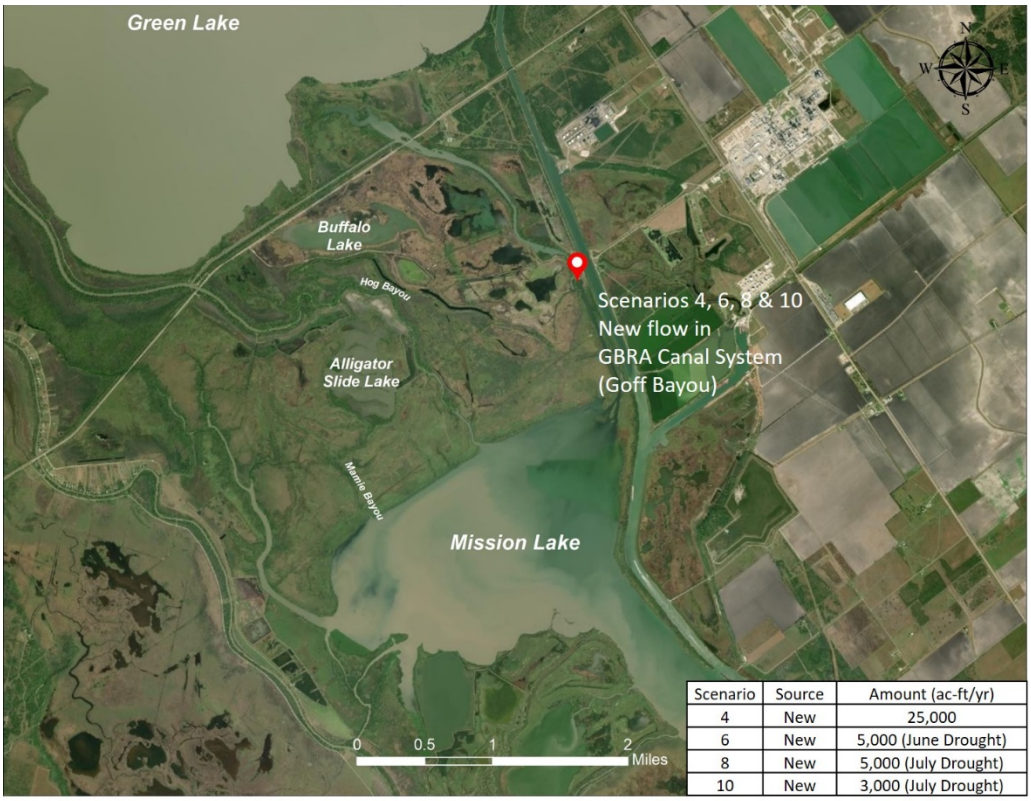

Figure 16. Scenario 4 diversion and scenarios 6, 8, and 10 additions

respectively. After review of the results of those two scenarios, the final four simulations were planned. Scenarios 7 and 8 simulated the impacts of the new 5,000 ac-ft applied in the month of July (81 cfs, 53 MGD) for the drought years at either Townsend Bayou or Goff Bayou, respectively. The new flows were reduced to 3,000 ac-ft for the month of July (49 cfs, 32 MGD) in the drought years at either Townsend Bayou or Goff Bayou in scenarios 9 and 10, respectively.

Each scenario simulation generated many different tabular and graphical output files, comprising too many to present in this report. Selected examples of the graphical results are presented as demonstrations of the local responses of the hydrodynamic SA Bay model. For reference, Figures 22 to 24 depict the freshwater river and bayou inflow locations for each scenario. Five locations were used in scenarios 1 (baseline), 4, 6, 8, and 10 as shown in Figure 22, with new flows added at Goff Bayou in the latter four simulations. Only scenario 2 included the Boat Canal as an additional inflow location with diversion from the Guadalupe River below Traylor's Cut, as shown in Figure 23. Scenarios 3, 5, 7, and 9 included Townsend Bayou as an additional inflow location. Scenario 3 considered diversion from the Guadalupe River above the Saltwater Barrier, while the latter three scenarios included only new flows introduced to Townsend Bayou.

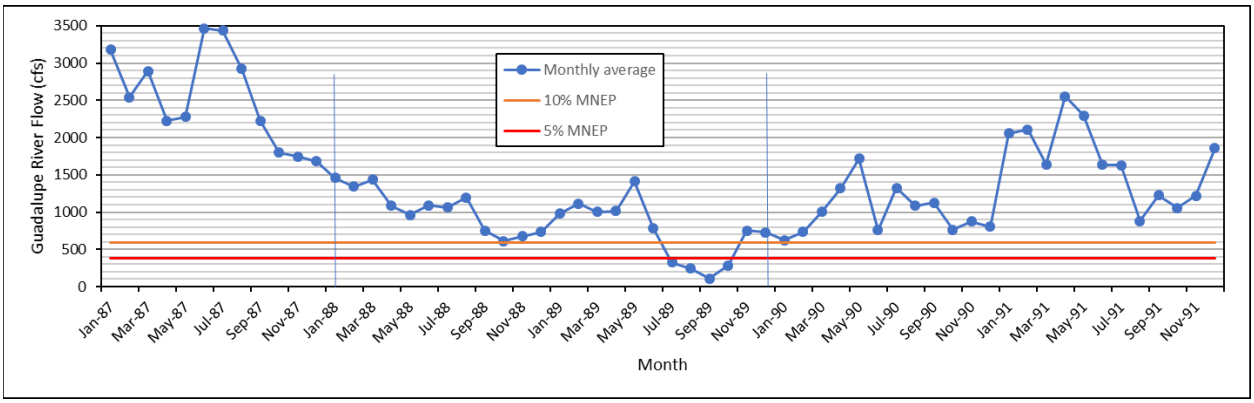

Figure 17. Guadalupe River flows around the 1988-89 drought

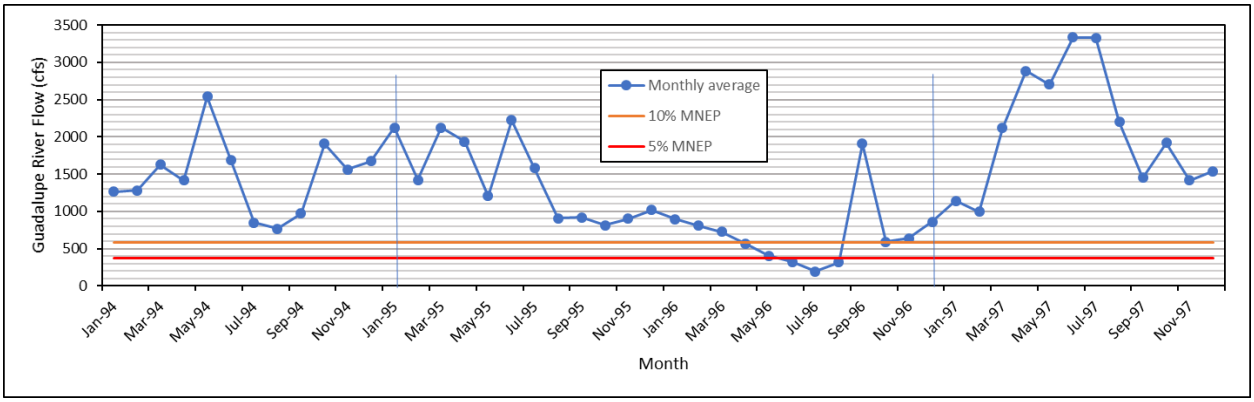

Figure 18. Guadalupe River flows around the 1995-96 drought

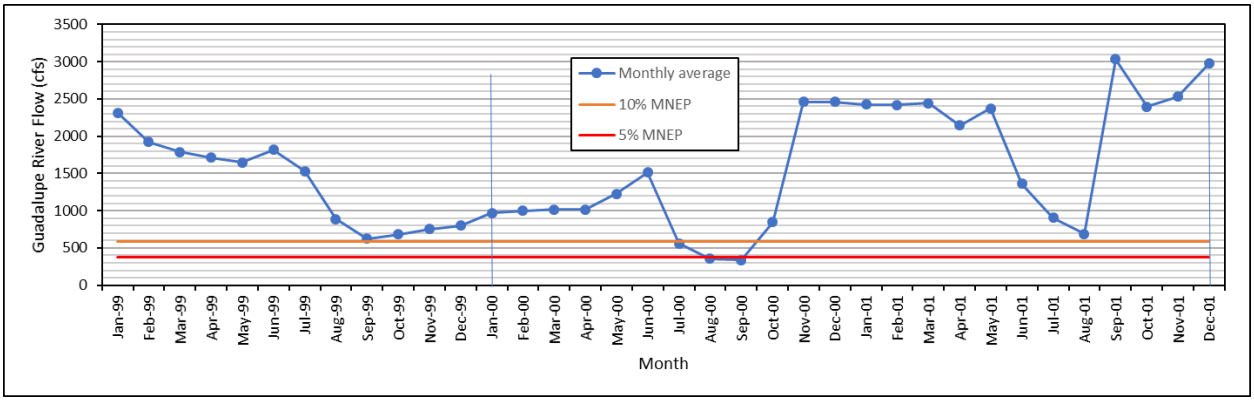

Figure 19. Guadalupe River flows around the 2000-01 drought

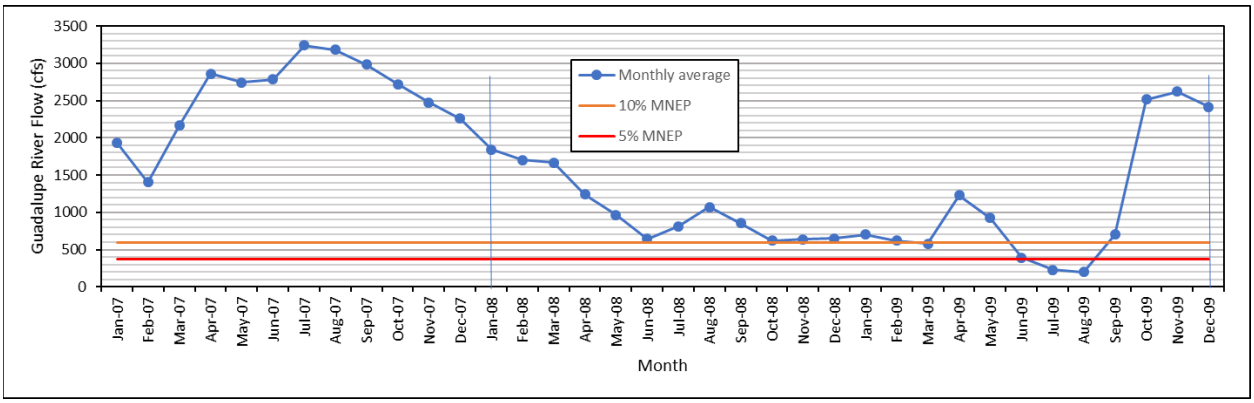

Figure 20. Guadalupe River flows around the 2008-09 drought

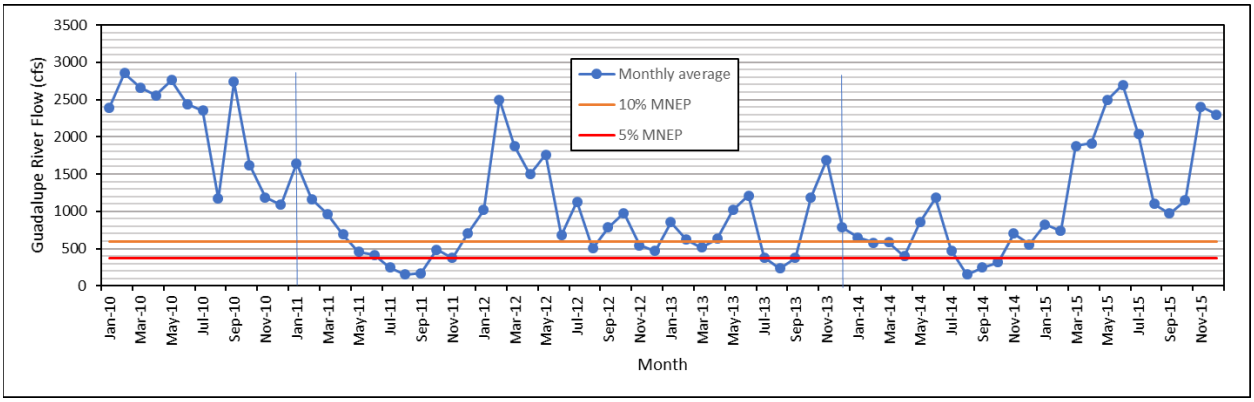

Figure 21. Guadalupe River flows around the 2011-13 drought

Examples from the baseline scenario 1 simulations were previously presented in the comparisons with observed salinity data in Figures 11 to 13. Additional freshwater inflow in the other scenarios was expected to cause some local reductions in salinity, but the model simulations were necessary to demonstrate the relative magnitudes of those effects. Scenarios 2, 3, and 4 included the larger freshwater changes at 10,000, 25,000, and 25,000 ac-ft/yr, respectively. Figure 24 provides a zoomed-in look at the simulated salinity variations for those three scenarios compared with the baseline scenario 1 during 2012. During most of the year, only the black line for the baseline is visible because all four lines are aligned. In the later months, the green line for scenario 4, the larger flow addition at Goff Bayou on the Seadrift side of the SA Bay domain, is often below the baseline due to the visible dilution effects. The blue line for scenario 3 is often above the baseline salinity plot, as loss of river water diverted to Townsend Bayou contributed to slightly increased salinity. Close inspection shows that the diversion of river water to the Boat Canal had a smaller impact as shown by the position of the red line. It must be noted that this location is not a primary target of freshwater encouragement of marsh vegetation, but the comparison does demonstrate that the SA Bay model is sensitive atthis position to the freshwater flow adjustments to the continually varying river and bayou inflows.

Figure 22. Freshwater inflow locations for scenarios 1, 4, 6, 8, and 10

Figure 23. Freshwater inflow locations for scenario 2

Figure 24. Freshwater inflow locations for scenarios 3, 5, 7, and 9

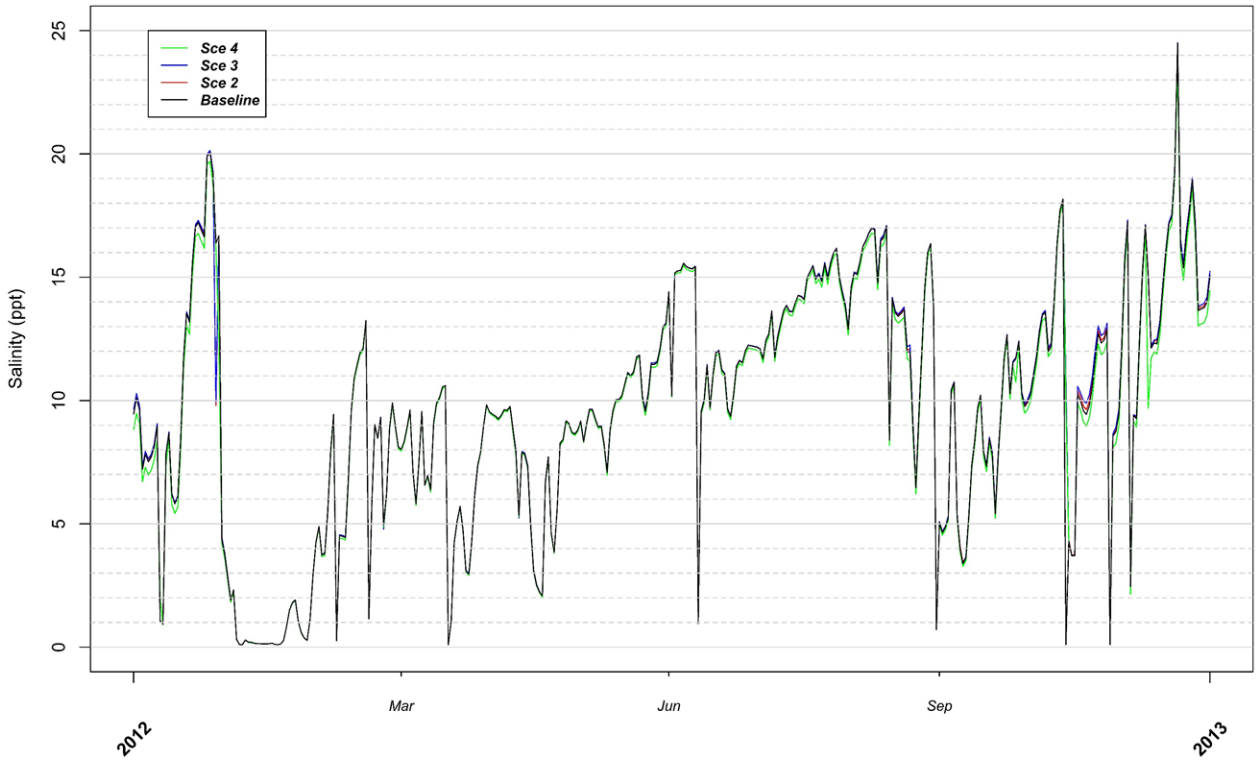

Figure 25. Salinities for scenarios 1, 2, 3, and 4 at node near Seadrift

The next sets of comparisons considered positions much closer to the mouths of the input channels for Townsend Bayou on the Hynes Bay side of the delta and Goff Bayou on the Mission Lake side. The depth and salinity variations simulated in the first multiyear drought of 1988-89 were considered in Figures 26 to 29. As shown in Figure 26, the depths at the Townsend Bayou mouth node varied from 0 to over 2 m. The lines for the baseline and scenarios 5, 7, and 9 are all often aligned under the red line. Scenario 3, the blue line, considered the year-round addition of flow, so the blue line is visible above the red line for most of the lowest baseline flow conditions. The lower flows for the month of June or July in scenarios 5, 7, and 9 had little effect on the depths. On the other hand, Figure 27 shows large salinity variations among the scenarios. Scenario 3 with the continuous freshwater addition, shown again as the blue line, caused great reductions in the salinity of this shallow water. Scenario 5 showed reduced salinity near the months of June, while scenario 7 was slightly effective near the month of July. Scenario 9 (red line) with the lower freshwater addition in July typically aligned with the baseline condition (black line under the red line). Simulated depths near the mouth of Goff Bayou ranged from about 0.6 m to almost 3 m during 1988-89 in the baseline scenario 1 as well as scenarios 4, 6, 8, and 10. All five scenario depth results are aligned in Figure 28, so the added flows were easily accepted by Mission Lake. Impacts of the added freshwater flows on salinity are shown in Figure 29. The larger flow addition for scenario 4 had the most often visible effect as represented by the blue line. The green and red lines for scenarios 6 and 8 show salinity reductions near June and July, respectively, as desired. The lower flow addition of scenario 10 was not enough to cause the salinity to differ from the baseline conditions.

The research team reviewed these and other SA Bay model results and judged them as acceptable demonstrations of the sensitivity of the TELEMAC-2D model. Pertinent outputs of the hydrodynamic simulations of each scenario were provided for input to the SA Bay EDYS ecohydrological model. Those simulations are discussed in the next section.

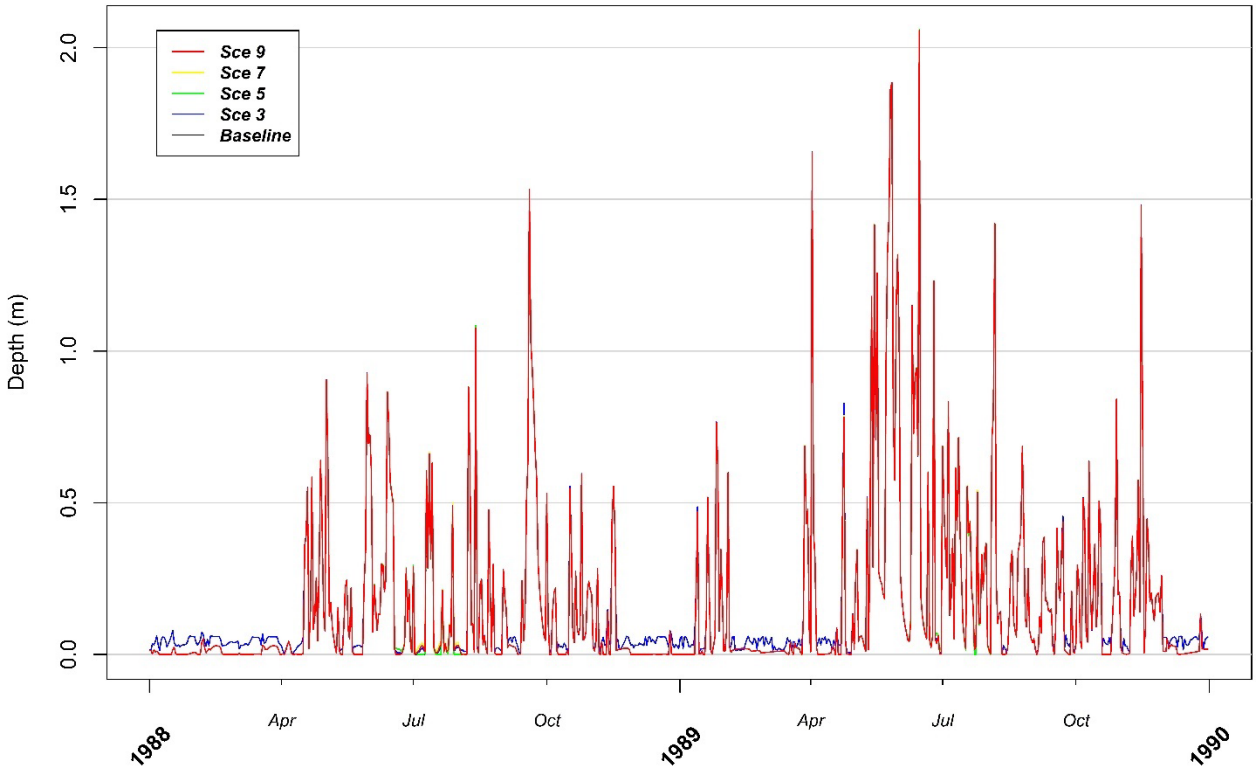

Figure 26. Depths for scenarios 1, 3, 5, 7, and 9 near mouth of Townsend Bayou, 1988-89

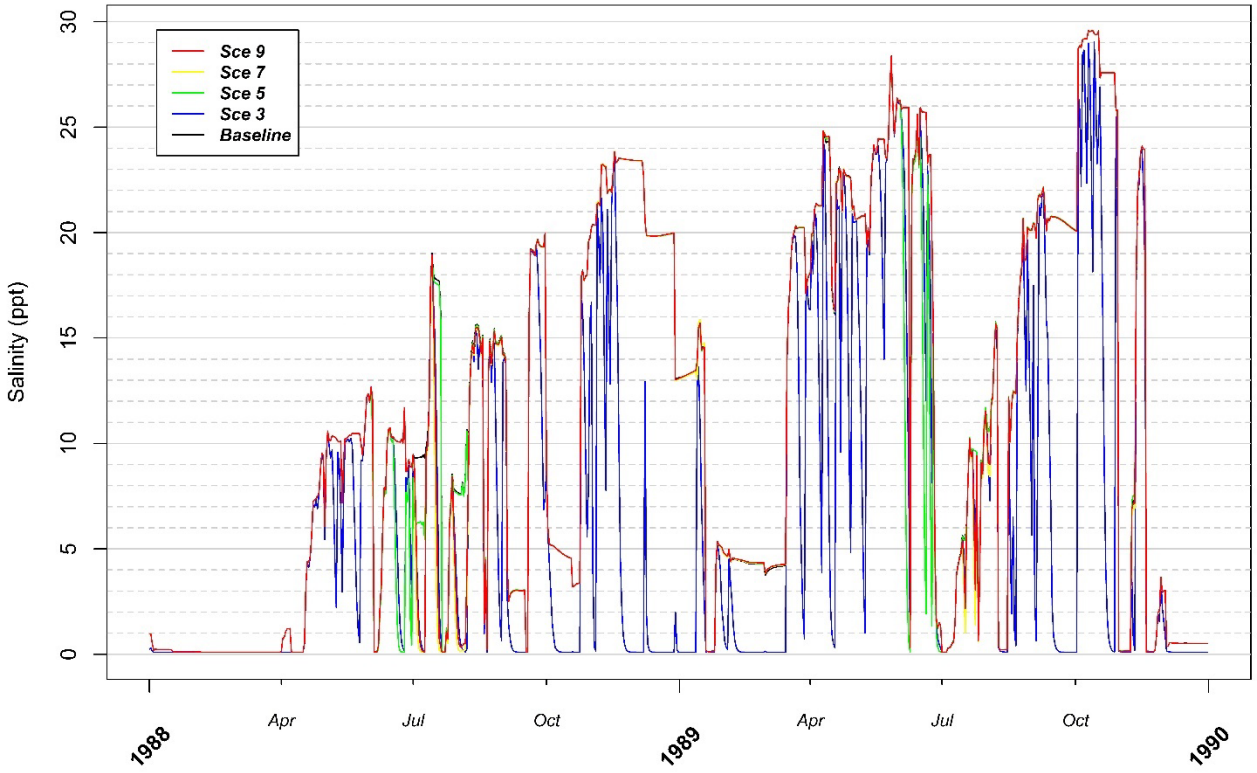

Figure 27. Salinities for scenarios 1, 3, 5, 7, and 9 near mouth of Townsend Bayou, 1988-89

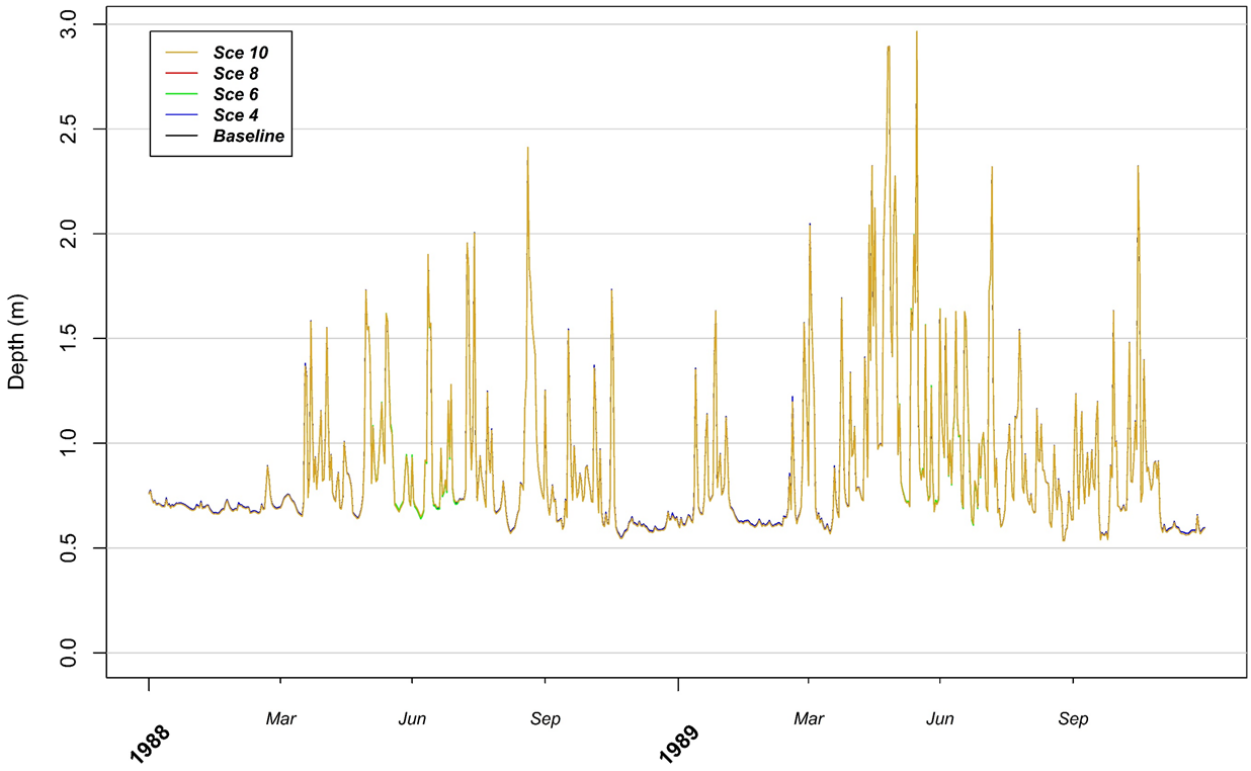

Figure 28. Depths for scenarios 1, 4, 6, 8, and 10 near mouth of Goff Bayou, 1988-89

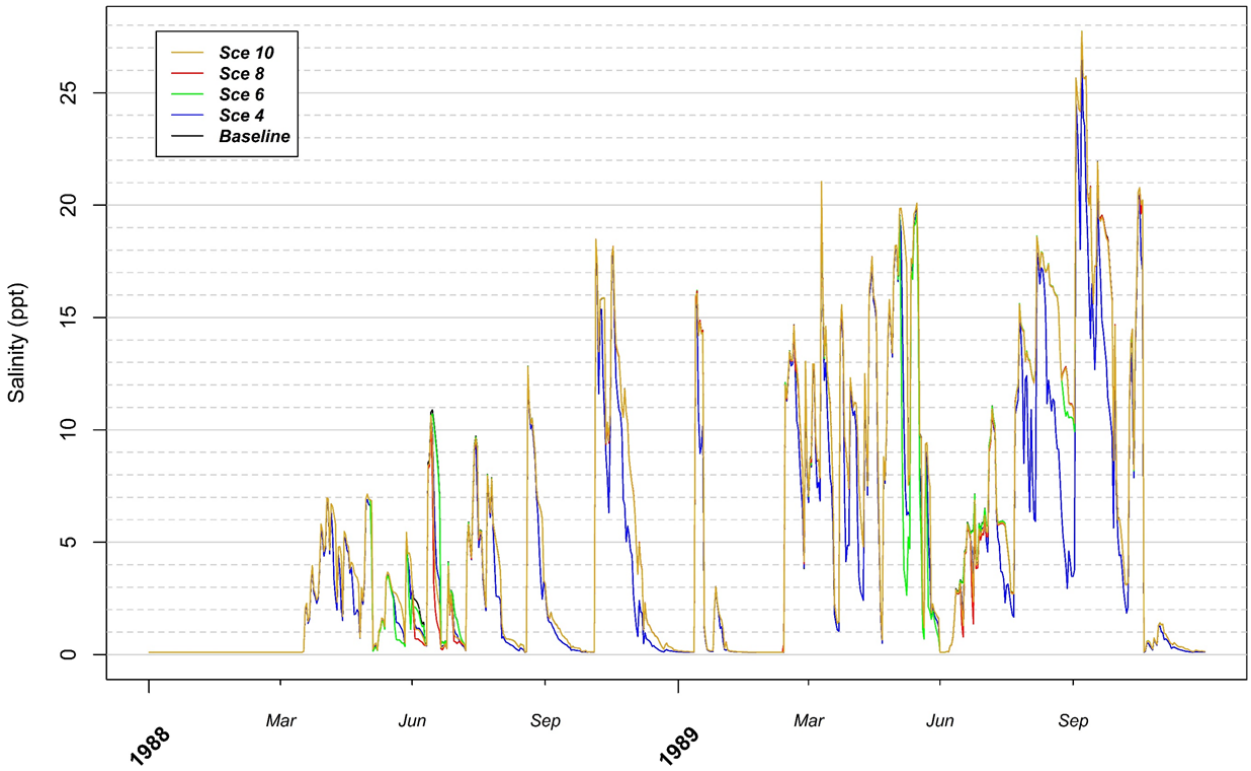

Figure 29. Salinities for scenarios 1, 4, 6, 8, and 10 near mouth of Goff Bayou, 1988-89

4 Linkage of EDYS with TELEMAC-2D

4.1 Domains and Linkage Steps

An EDYS application was developed for the entire San Antonio Bay, as shown in Figure 30. This model included 2.79 million cells, 395 plot types (which we define as unique combinations of vegetation and soils), 74 plant species, and 72 soil profiles. The full list of plant species can be found in Appendix A.

Figure 30. Full domain extent for EDYS Model for San Antonio Bay

The design of EDYS allows the tracking of changes in plot types over time, giving it the flexibility to simulate plant, soil, and water dynamics in great detail spatially. Unfortunately, the Windows operating system in which EDYS runs forces limits on heterogeneity that can be simulated. We recognize that salinity and water depth vary across the bay, from north to south, and from east to west. Consequently, we were not able to link the EDYS application for the full domain with TELEMAC-2D.

In order to capture heterogeneity in salinity and depth across the bay, we subdivided the coastal zone into eight regions, and created a separate EDYS model for each. The coastal shore boundaries of the eight small EDYS models are shown in Figure 31. Inland, each model extended approximately 1000 m from open water, except for the model encompassing the Delta, which had no inland limit and covered the entire extent of the Delta.

Figure 31. Spatial extent of small EDYS models with black lines as approximate boundaries between small models

As a result, the linkage process for simulation runs with EDYS and TELEMAC-2D followed these steps.

1. The full domain EDYS model application was run for the period of record, 1987-2013. Surface runoff data were tallied on an event basis for each TELEMAC-2D node on the boundary, and output to a file.
2. TELEMAC-2D was run for each freshwater inflow scenario using the runoff output data generated in Step 1 for the full domain EDYS model. An output file containing water depth and salinity level was generated for each TELEMAC-2D node on the boundary and on the Delta.
3. Each of the eight small-scale EDYS models were run using depth and salinity outputs generated by TELEMAC-2D.

4.2 Measures for Comparison

In order to evaluate potential impacts of each freshwater inflow scenario, the following ratio was calculated on an annual basis for each plant community in each of the eight small-scale EDYS models:

$$Ratio = \frac{Scenario\ Biomass}{Baseline\ Biomass} \quad (2)$$

A ratio value that exceeded 1.0 represented a situation where the scenario outcome was an improvement over baseline conditions, while a value less than 1.0 represented a case where biomass production fell below the baseline conditions. A value of 1.0 represented no change in biomass from baseline. Throughout the remainder of this report, ratios greater than 1.0 will be called "Positive", "Negative" refers to ratios less than 1.0, and "Even" are for ratios of 1.0. This nomenclature assumes that increases in submerged vegetative biomass are desirable as refugia for the larval stages of various organisms, while decreases in submerged biomass will be detrimental to those organisms, although we did not distinguish between submerged and un-submerged biomass.

There are multiple hierarchical approaches that could be taken to evaluate the impacts of the different scenarios on vegetation. These approaches include total aboveground biomass for all species within a community, total aboveground biomass for desirable species within each community, total aboveground biomass for undesirable species, and the spatial extent of Positive-Even-Negative for different regions of the bay. The primary focus for the remainder of this report will be on community-level total aboveground biomass, as well as the spatial extent in areas near release points, in zones of influence.

Desirable species within low lying, tidally influenced communities, based on our validation sampling in the bay (McLendon et al. 2020) include the following: inland saltgrass (*Distichlis spicata*), marshhay cordgrass (*Spartina patens*), smooth cordgrass (*Spartina alterniflora*), and Olney bulrush (*Schoenoplectus americanus*). The undesirable species of interest is common reed (*Phragmites australis*). Dynamics of individual species are included in Appendix B.

5 Vegetative Responses to Hydrological Changes

5.1 Scenario 2

The spatial extent of Positive-Even-Negative for Scenario 2, the diversion of 10,000 ac-ft/yr from Guadalupe River below Traylor's Cut to the Boat Canal on the Delta, is shown in Figure 32. There are some benefits in the Delta to the additional water, but it is not universally seen across the Delta, with 27.6 percent of the Delta experiencing negative ratios (Table 3). Additionally, the loss of freshwater flowing into Mission Lake from the river has a

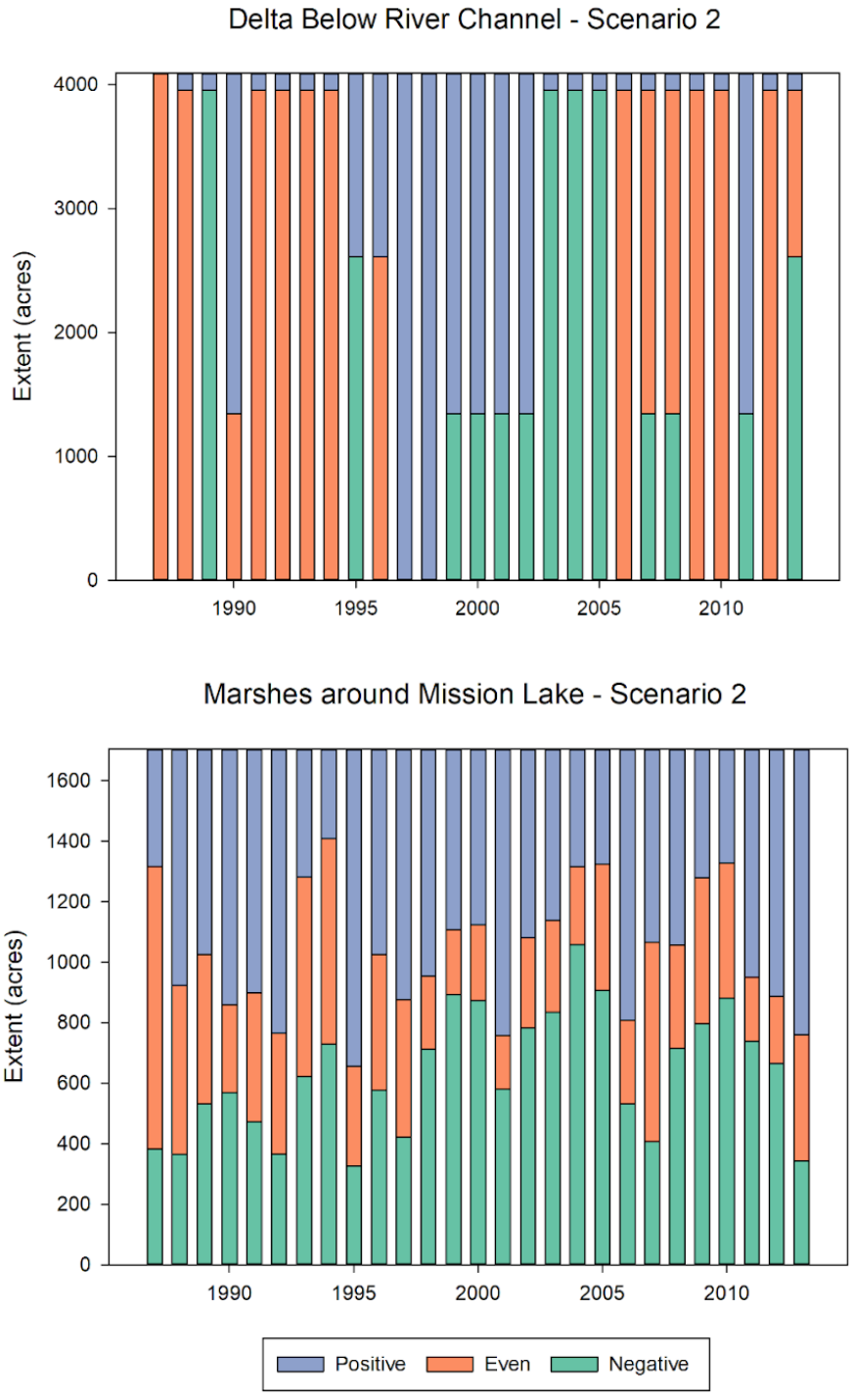

Figure 32. Vegetative responses for scenario 2

Table 3. Mean Spatial Extents of Vegetative Responses for Scenario 2

Biomass Ratio	Mean Acreage (%)	
	Delta	Mission Lake
Positive	1104.9 (27.0)	669.8 (39.3)
Even	1859.5 (45.4)	403.1 (23.6)
Negative	1127.6 (27.6)	632.6 (37.1)

substantial impact on the salt marshes lining Mission Lake. An average of 37.1 percent of the acreage in salt marsh showed declines, indicating there was a tradeoff between different parts of the bay as a result of the diversion from the river.

5.2 Scenario 3

Scenario 3 is the diversion of 25,000 ac-ft/yr from the Guadalupe River above the GBRA Saltwater Barrier and releasing it where Townsend Bayou intersects Highway 35, allowing the water to flow overland to Hynes Bay. As seen in Figure 33, the vast majority of the area below the release point experienced a positive impact from the additional flows, with only 6.5 percent of the area being negatively impacted. On the other hand, the diversion resulted in declines in biomass on both the Delta (53.2 percent) and the salt marshes surrounding Mission Lake (63.1 percent), as shown in Table 4.

Table 4. Mean Spatial Extents of Vegetative Responses for Scenario 3

Biomass Ratio	Mean Acreage (%)		
	Townsend Bayou	Delta	Mission Lake
Positive	2833.5 (91.9)	784.4 (19.2)	431.2 (25.3)
Even	47.8 (1.6)	1129.4 (27.6)	198.0 (11.6)
Negative	201.0 (6.5)	2178.2 (53.2)	1076.4 (63.1)

5.3 Scenario 4

Scenario 4 is the addition of 25,000 ac-ft/yr of water in Goff Bayou, with no diversions from the river. Not surprisingly, substantial benefits were seen in the salt marshes lining Mission Lake (Figure 34 and Table 5). Interestingly, almost 24 percent of the Delta experienced negative impacts of this additional water, which seems counterintuitive. A deep investigation into one of the impacted communities reveals a logical explanation. This community was a mixture of only four species, inland saltgrass, smooth cordgrass, Olney bulrush, and widgeon grass (*Ruppia maritima*). On April 11, 1987, one of the nodes in TELEMAC-2D that supplied water to this community went dry, resulting in a reduced uptake of water by three of the species (saltgrass, cordgrass, and bulrush). Consequently, production was reduced in those species, and that reduction was propagated throughout the remainder of the growing season. Ultimately, the ratio

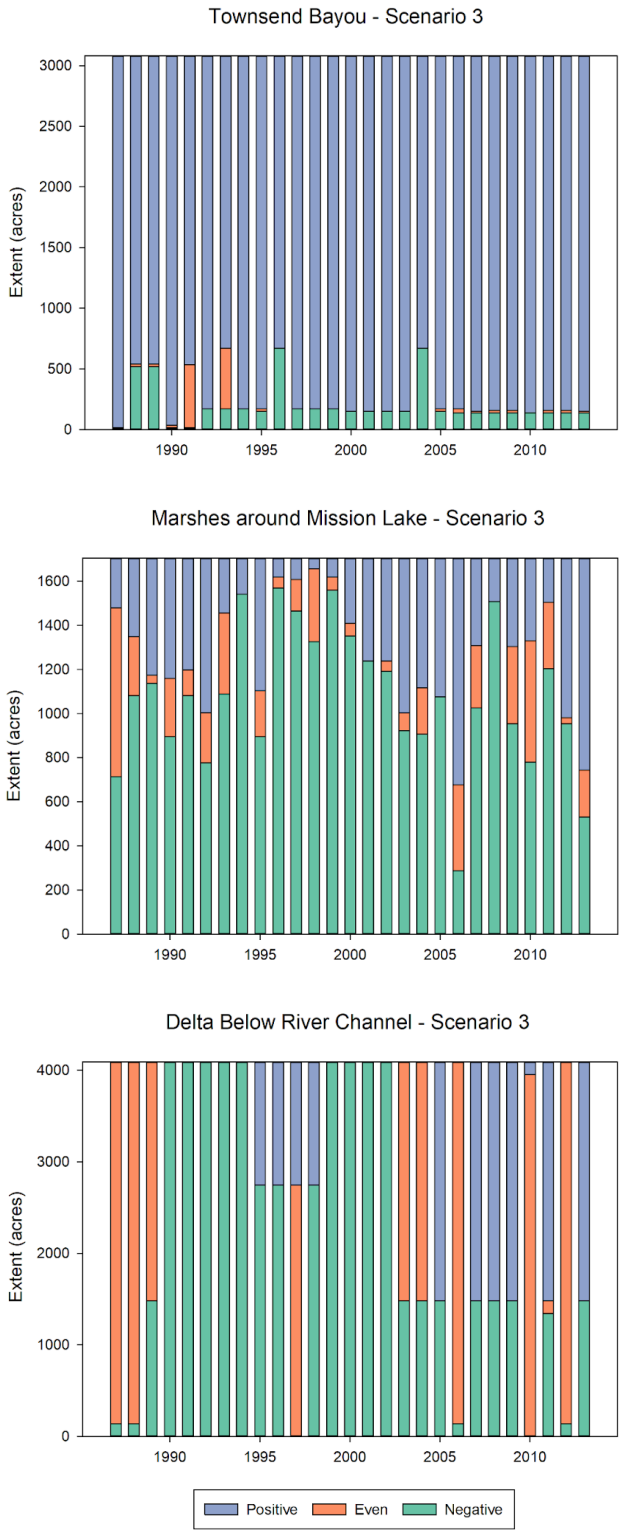

Figure 33. Vegetative responses for scenario 3

for that year was less than 1.0.

Comparing the water depth at that node in the TELEMAC-2D between this scenario and baseline revealed that the depth of water at baseline was less than 10 cm. It is possible the inter-node distance was too great for TELEMAC-2D to capture that degree of variability, and it is also possible the result was an accurate representation of flows in that area, even with the addition of water. Substantial time and effort beyond the current project scope would be required to resolve the reasoning behind why the node went dry. However, given that issue, the vegetative responses are accurate and reflect the hydrological differences of the inputs.

Table 5. Mean Spatial Extents of Vegetative Responses for Scenario 4

Biomass Ratio	Mean Acreage (%)	
	Mission Lake	Delta
Positive	1198.1 (70.3)	1615.6 (39.5)
Even	92.7 (5.4)	1500.3 (36.7)
Negative	414.7 (24.3)	976.1 (23.8)

5.4 Scenarios 5, 7, and 9

Scenarios 5, 7, and 9 were grouped together for comparison because each of these involve additional water being applied in Townsend Bayou with overland flow to Hynes Bay during drought years only (1988-1989, 1995-1996, 2000-2001, 2008-2009, and 2011-2013). Scenario 5 was 5,000 ac-ft added in June, scenario 7 was 5,000 ac-ft added in July, while scenario 9 was 3,000 ac-ft added in July. Figure 35 shows average acreage across all five drought periods and the changes in impact in successive years of the drought. Please note that only one drought extended across three years (2011-2013), so the acreage for year 3 in the figure was based only on one sample point.

With the addition of water in June (scenario 5), the amount of acreage experiencing negative impacts declined in each successive drought year. When water was added in July, there were increases in negative impacts from year 1 to year 2, on average. The impacts were reduced with 3,000 ac-ft as opposed to 5,000 ac-ft.

5.5 Scenarios 6, 8, and 10

As with scenarios 5, 7, and 9, the results for scenarios 6, 8, and 10 were shown together because they involved releases of additional water in Goff Bayou during drought years only (1988-1989, 1995-1996, 2000-2001, 2008-2009, and 2011-2013). Scenario 6 was 5,000 ac-ft added in June, scenario 8 was 5,000 ac-ft added in July, while scenario 10 was 3,000 ac-ft added in July. The zone of influence for those releases included the salt marsh communities surrounding Mission Lake. Scenario 6 (Figure 36) resulted in increases in the average area experiencing negative impacts in successive years. That pattern did not hold for releases in

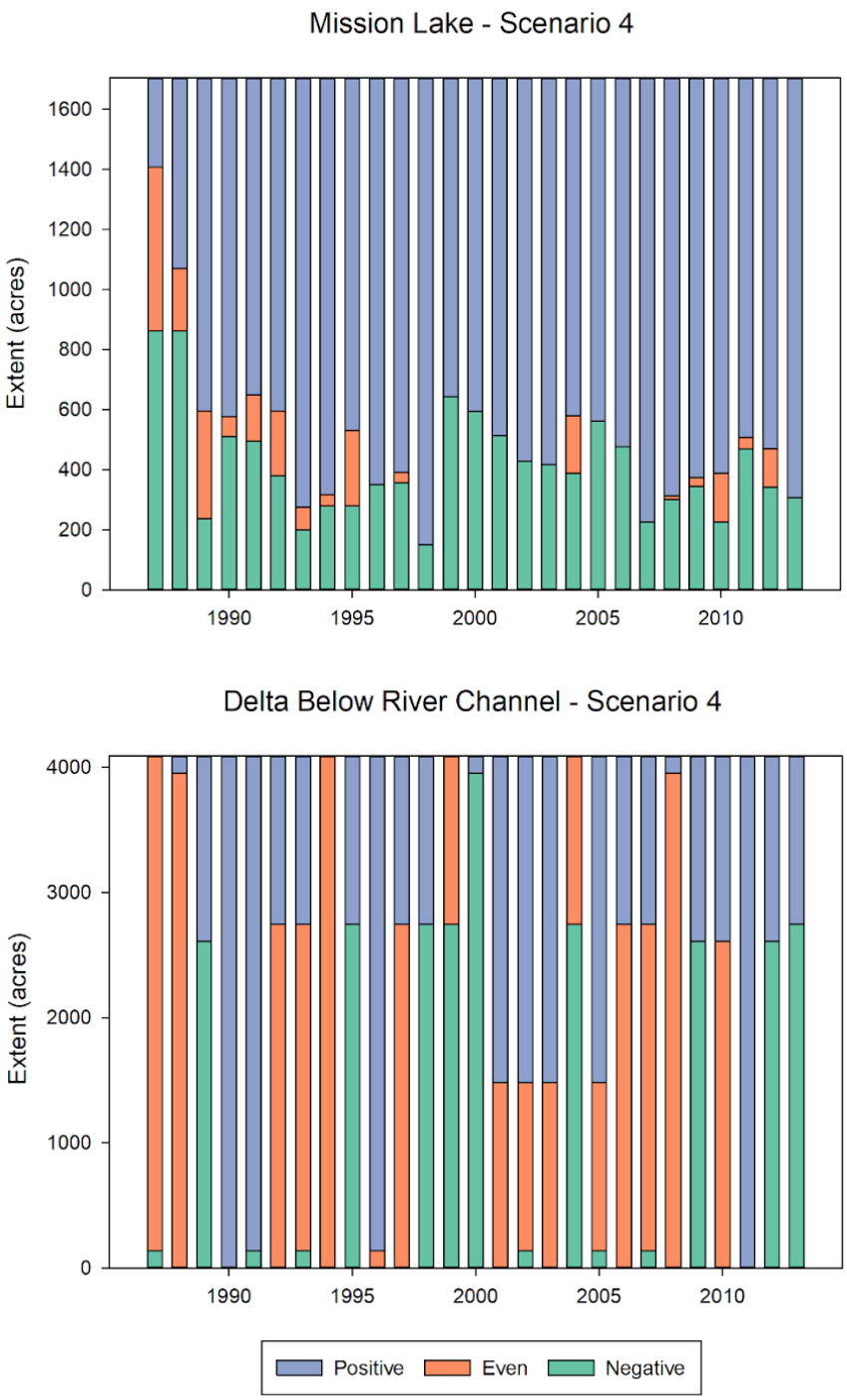

Figure 34. Vegetative responses for scenario 4

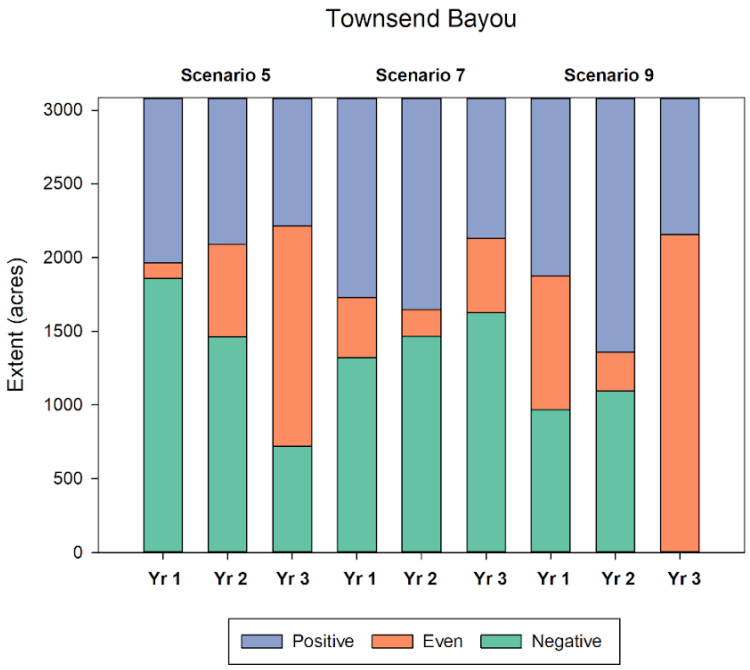

Figure 35. Average vegetative response south of the release point in Townsend Bayou during drought years for scenarios 5, 7, and 9 for drought years 1988-1989, 1995-1996, 2000-2001, 2008-2009, and 2011-2013

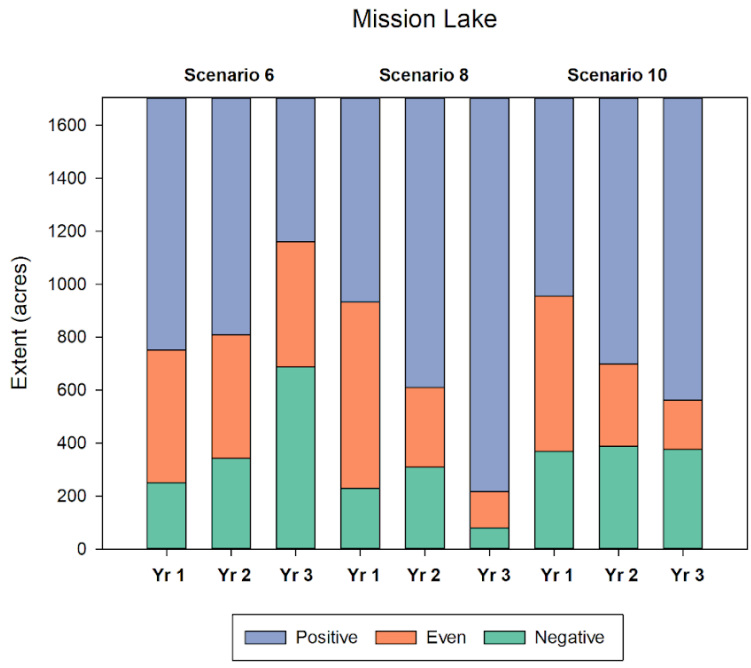

Figure 36. Average vegetative response of salt marshes lining Mission Lake during drought years for scenarios 6, 8, and 10 for drought years 1988-1989, 1995-1996, 2000-2001, 2008-2009, and 2011-2013

July, for both 5,000 and 3,000 ac-ft. In fact, the amount of acreage experiencing positive impacts increased in successive years. The amount of water released seemed to have an impact with July releases. The spatial extent of negative impacts was less with 5,000 ac-ft than with 3,000 ac-ft.

For scenarios 5-10, the results presented in Sections 5.4 and 5.5 showed average acreage across all drought periods. However, results from individual drought periods can be instructive for understanding finer temporal scales and their potential impacts on management of water flows. For example, consider the differences in vegetation responses during the droughts of 1995-1996 (Figure 37) and 2000-2001 (Figure 38) for releases in Goff Bayou. During the drought of 1995-1996, the spatial extent of negative impacts increased from year 1 to year 2 in all three scenarios (6, 8, and 10). Contrast that finding with the responses during the drought of 2000-2001, particularly for scenarios 8 and 10. The extent of negative impacts decreased in year 2 for both of those scenarios. The reasons behind these differences lie in the changes in river flows between the releases. In 1995-1996, river flows did not rebound in any appreciable manner (Figure 37), while river flows increased during winter months in the middle of the 2000-2001 drought (Figure 38). Apparently, the increased river flows in 2000-2001 allowed for greater vegetative maintenance, resulting in lower negative impacts in year 2. This finding has potential management implications regarding the magnitude of additions needed in the second year of the drought. It is possible that less water is needed in year 2 following a rebound in river flows. Determining that threshold level would require additional simulation runs.

6 Conclusions

6.1 Scenario Simulations with the Ecohydrological and Hydrodynamic Models

Vegetation dynamics in EDYS, linked with TELEMAC-2D, responded to changes in freshwater inflows in reasonable patterns. Higher flow volumes tended to produce the greatest positive impacts in zones of influence near release points, illustrating the potential value of increased freshwater inflows. However, diversions from the Guadalupe River also resulted in trade-offs between different parts of the bay system. For example, when water was diverted into Townsend Bayou, the salt marshes lining Mission Lake were detrimentally impacted by the lower flows coming from the river. The same result was seen with the diversion into the Boat Canal, with vegetation in the salt marshes around Mission Lake being negatively impacted. Whether those trade-offs are acceptable is beyond the scope of this modeling effort.

The addition of added freshwater during periods of drought revealed several patterns of interest when considering potential management in the bay. The additional water was added under the assumption that increased inflows would serve to support the existing vegetation, allowing it to maintain itself during the drought. The simulations revealed that several factors are important when considering these additions. In some cases, the timing of release was important, with plant communities located north of Hynes Bay responding better to releases in June, while the salt marshes around Mission Lake responded more positively to releases in July.

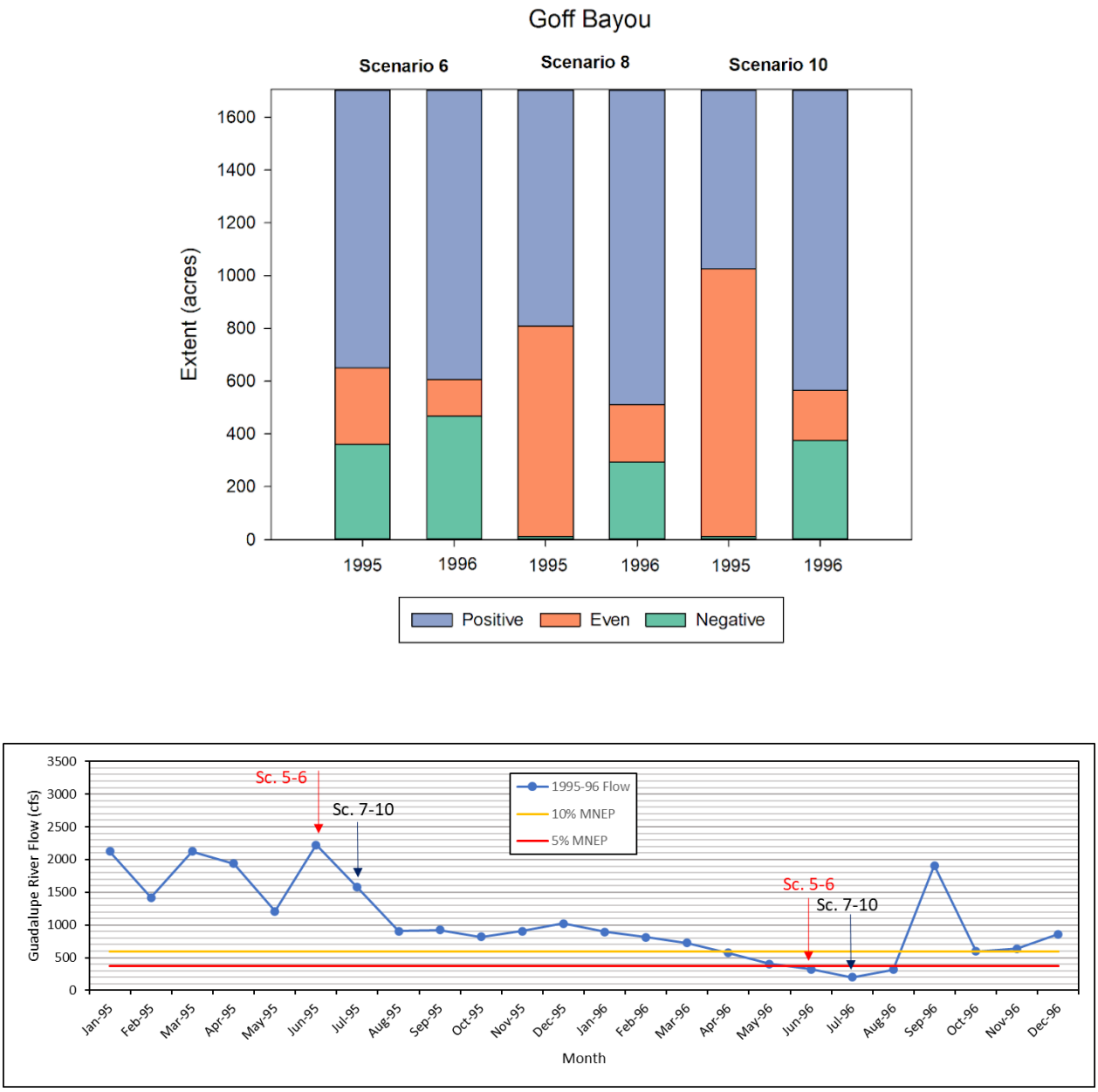

Figure 37. Vegetative responses to drought in 1995-1996 showing average extent for salt marshes lining Mission Lake by year (top) compared to flows in the Guadalupe River and timing of releases in Goff Bayou (bottom)

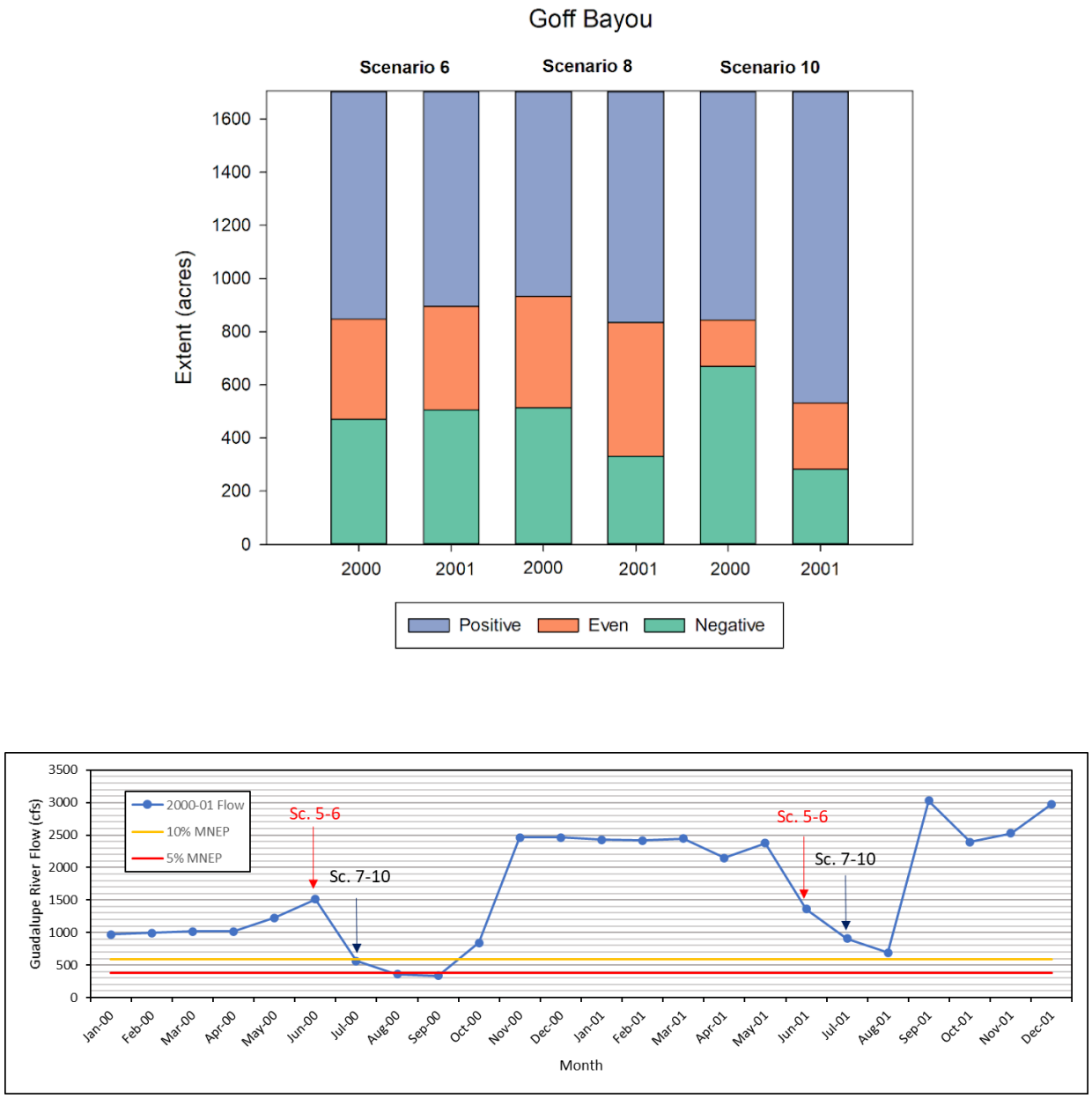

Figure 38. Vegetative responses to drought in 2000-2001 showing average extent for salt marshes lining Mission Lake by year (top) compared to and flows in the Guadalupe River and timing of releases in Goff Bayou (bottom)

The magnitude of releases tended to be related to vegetative responses, with more positive impacts seen with 5,000 ac-ft than 3,000 ac-ft. However, a closer look at flow patterns in the Guadalupe River during droughts, and between releases, shows that potential recovery of river flows may have an impact on the magnitude and timing of additional freshwater needed for maintenance of the vegetation. Further simulations are needed to more fully elucidate the most effective timing and amounts of added freshwater flows for vegetation maintenance.

6.2 Completion of Project Scope of Work

This work is part of a larger set of tasks that began in 2011 to address the needs of the River Authority for effective simulation of watershed conditions and water and salinity circulation near the San Antonio Bay. The EDYS ecohydrological model has been successfully demonstrated for simulation of watershed conditions along the San Antonio and other rivers, as well as for watersheds adjacent to the San Antonio Bay. Apart from the current study, the finely calibrated EDYS model has compared well with six years of validation sampling from 2014-2019, and an additional sampling round is planned for 2020. The project requirements for bay circulation simulation were met through application of the TELEMAC-2D hydrodynamic model that successfully simulated salinity, depth, and velocity conditions in our SA Bay model. With using limited available spatial and temporal data, the TELEMAC-2D model results compared reasonably well with limited salinity records at three SA Bay observation sites, and the simulation results were sensitive to changes in freshwater inflows. The EDYS and TELEMAC models were successfully coupled for simulation of multiple "what-if" scenarios to evaluate impacts of freshwater inflows on vegetation distributions in the marsh areas. The tools are ready for additional applications.

6.3 Thoughts for Future Applications

As intended by the River Authority staff, the EDYS-TELEMAC-2D models for San Antonio Bay can be applied to test different ecological management strategies based on the introduction of freshwater at selected locations and timing to demonstrate impacts of changes in salinity and water depth on vegetation. If necessary, the discretization of TELEMAC-2D can be adjusted for more precise descriptions of critical target locations. The research team is ready to pursue future applications while teaming with the River Authority and other appropriate water agencies and stakeholder groups. Effective partnerships are needed to define desired biomass targets for specific vegetation species and the locations at which those targets are most useful. On the engineering and hydrologic sides, realistic new or diverted water sources must be identified as well as appropriate delivery locations relative to those target vegetation species. In a larger sense, the combination of the EDYS models for the counties along the San Antonio and Guadalupe rivers with the EDYS and TELEMAC-2D models for the San Antonio Bay vicinity represent the type of simulation tools necessary for regional-scale discussions of desired environmental flow conditions.

7 References

Ata, R. 2020. Telemac2d User Manual, Version v8p1, Electricite de France, accessed from http://www.opentelemac.org/, 124 p.

Guthrie, C.G., Matsumoto, J., and Lu, Q. 2010. TxBLEND Model Calibration and Validation for the Guadalupe and Mission-Aransas Estuaries, Bays and Estuaries Program, Surface Water Resources Division, Texas Water Development Board, Austin, Texas, 46 p.

Hervouet, J. 2007. Hydrodynamics of Free Surface Flows: Modelling with the Finite Element Method, Wiley Publishers, West Sussex, England, 319 p.

Mattic, O. 2020a. Telemac2d Reference Manual, Version v8p1, Electricite de France, accessed from http://www.opentelemac.org/, 110 p.

McLendon, T., Booker, J., Coldren, C., Pappas, C., and Swinehart, J. 2015. Development of an EDYS Ecological Model of the Central San Antonio River Watershed: Karnes and Wilson Counties, Final Report for San Antonio River Authority, Texas Tech University, Lubbock, Texas, 223 p.

McLendon, T., Booker, J., Coldren, C., and Pappas, C. 2016. Development of an EDYS Ecological Model for Goliad County, Texas, Final Report for San Antonio River Authority and Texas State Soil and Water Conservation Board, Texas Tech University, Lubbock, Texas, 242 p.

McLendon, T., Booker, J., Coldren, C., Moberly, C., and Rainwater, K. 2018. Development of an EDYS Ecological Model for Victoria County, Texas, Final Report for San Antonio River Authority and Texas State Soil and Water Conservation Board, Texas Tech University, Lubbock, Texas, 275 p.

McClendon, T., Pappas, C., Coldren, C., Fish, E., Beierle, M., Hernandez, E., Rainwater, K., and Zartman, R. 2012. Application of the EDYS Decision Tool for Modelling of Target Sites for Water Yield Enhancement through Brush Control, Final Report for Texas State Soil and Water Conservation Board, San Angelo, Texas, 36 p.

McLendon, T., Stanley, K.S, and Stanley, K.D. 2020. San Antonio Bay EDYS Model Validation Study: Field Sampling Results 2014-2019, Final Report for San Antonio River Authority, Texas Tech University and KS2 Ecological Field Services, LLC., Lubbock and Anton, Texas, 71 p.

Robel, J. 2019. Personal communication, hourly wind data for Rockport Aransas County Airport, Texas GHCND:USW00012972 (28.08361°, -97.04639°), National Climatic Data Center, Asheville, NC, email data link transfer.

Texas Water Development Board, 2019. Lake Evaporation and Precipitation, Quadrangle 911, https://waterdatafortexas.org/lake-evaporation-rainfall, accessed March 2019.

Thompson, K. 1987. Time Dependent Boundary Conditions for Hyperbolic Systems, Journal of Computational Physics, Vol. 68, pp. 1-24.

Appendices

Appendix A. Plant species simulated in the EDYS model application for San Antonio Bay

Scientific Name	Common Name
Trees, Shrubs, and Cacti	
Acacia farnesiana	huisache
Celtis laevigata	sugar hackberry
Persea borbonia	sweetbay
Prosopis glandulosa	mesquite
Quercus virginiana	live oak
Baccharis halimiflora	sea myrtle
Borrichia frutescens	sea oxeye
Celtis pallida	granjeno
Lycium carolinianum	Carolina wolfberry
Rosa bracteata	McCartney rose
Sesbania drummondii	rattlepod
Vitis mustangensis	mustang grape
Opuntia lindheimeri	Texas prickly pear
Grass and Grass-like	
Andropogon gerardii	big bluestem
Andropogon glomeratus	bushy bluestem
Aristida purpurescens	arrowflower threeawn
Bothriochloa saccharoides	silver bluestem
Buchloe dactyloides	buffalograss
Cenchrus incertus	sandbur
Cynodon dactylon	bermudagrass
Distichlis spicata	saltgrass
Elionurus tripsacoides	Pan-American balsamscale
Leersia hexandra	clubhead cutgrass
Monanathochloe littoralis	shoregrass
Panicum hemitomon	maidencane
Panicum virgatum	switchgrass
Paspalum lividum	longtom
Paspalum monostachyum	gulfdune paspalum
Paspalum plicatulum	brownseed paspalum
Paspalum setaceum	thin paspalum
Paspalum vaginatum	seashore paspalum
Phragmites australis	common reed
Schizachyrium scoparium	sea coast bluestem
Setaria geniculata	knotroot bristlegrass
Setaria leucopila	plains bristlegrass
Sorghum bicolor	milo

Sorghum halepense	Johnsongrass
Spartina alterniflora	smooth cordgrass
Spartina patens	marshhay cordgrass
Spartina spartinae	gulf cordgrass
Sporobolus virginicus	seashore dropseed
Stipa leucotricha	Texas wintergrass
Uniola paniculata	sea oats
Zizaniopsis miliacea	marsh millet
Cyperus odoratus	flatsedge
Eleocharis interstincta	spikerush
Ruppia maritima	widgeon grass
Scirpus americanus	Olney bulrush
Typha latifolia	cattail

Forbs

Alternanthera philoxeroides	alligatorweed
Ambrosia psilostachya	ragweed
Aster spinosus	spiny aster
Baltis maritima	saltwort
Baptistia leucophaea	whitestem wild indigo
Chamaecrista fasciculata	partridge pea
Clematis drummondii	old-man's beard
Croton punctatus	gulf doveweed
Erigeron myrionactis	Corpus Christi fleabane
Eupatorium odoratum	mistflower
Gaillardia pulchella	indian blanket
Helianthus annuus	sunflower
Heterotheca subaxillaris	camphorweed
Ipomoea pes-caprae	railroad vine
Iva annua	seacoast sumpweed
Nelumbo lutea	lotus
Phyla nodiflora	frogfruit
Ratibida columnifera	prairie coneflower
Rhynchosia texana	snoutbean
Rumex crispus	curly dock
Sagittaria falacata	bulltongue
Salicornia virginica	glasswort
Sarcostemma cynanchoides	twinevine
Suaeda linearis	sea blite

Appendix B. Community responses and individual plant species responses to additional releases during drought periods

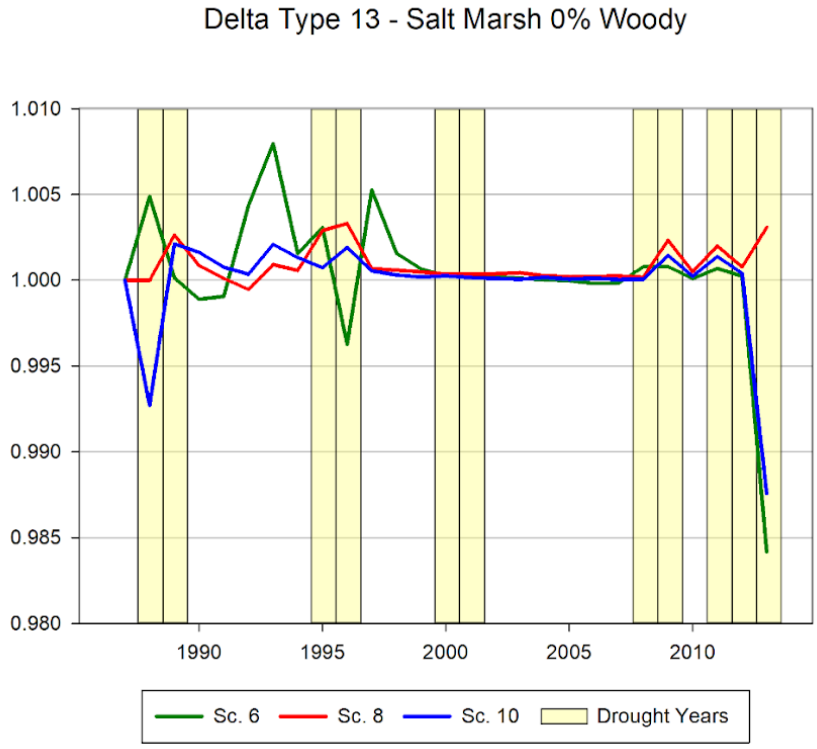

Figure B-1. Total aboveground biomass response for salt marsh, 0 percent woody community for scenarios 6, 8, and 10 (top) and location of this plant community (bottom)

Figure B-2. Total aboveground biomass response for salt marsh, 5 percent woody community for scenarios 6, 8, and 10 (top) and location of this plant community (bottom)

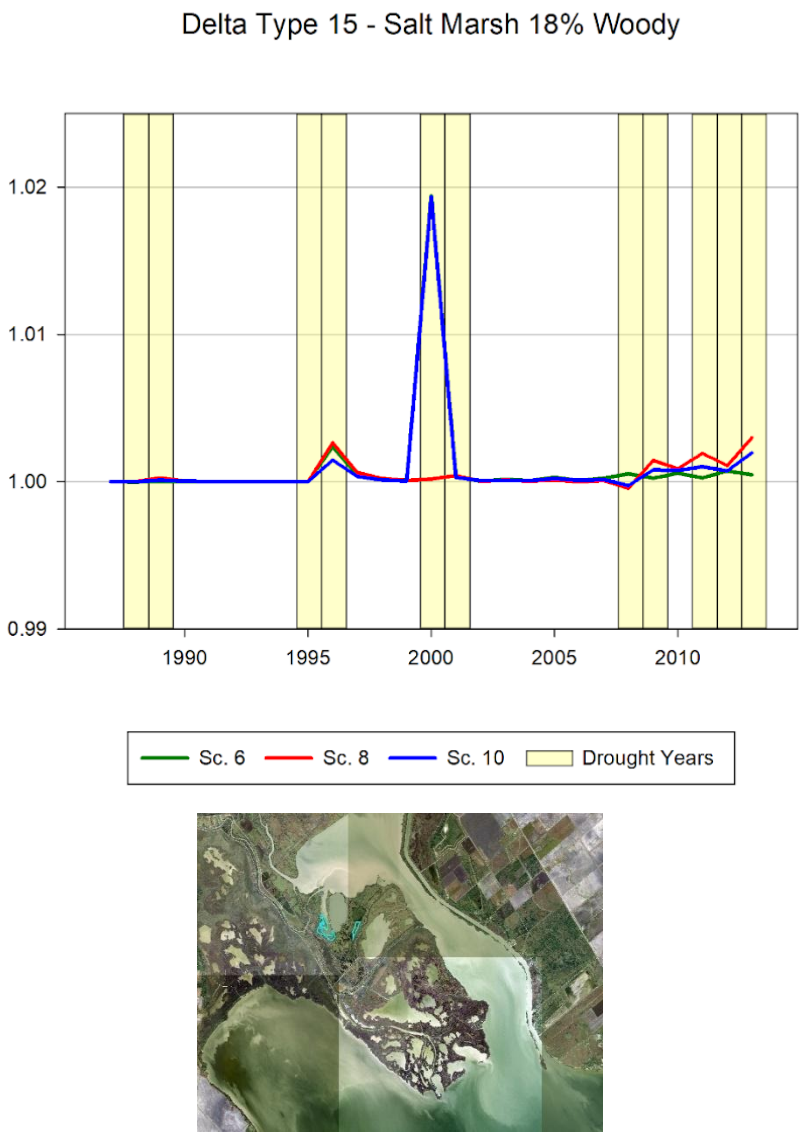

Figure B-3. Total aboveground biomass response for salt marsh, 18 percent woody community for scenarios 6, 8, and 10 (top) and location of this plant community (bottom)

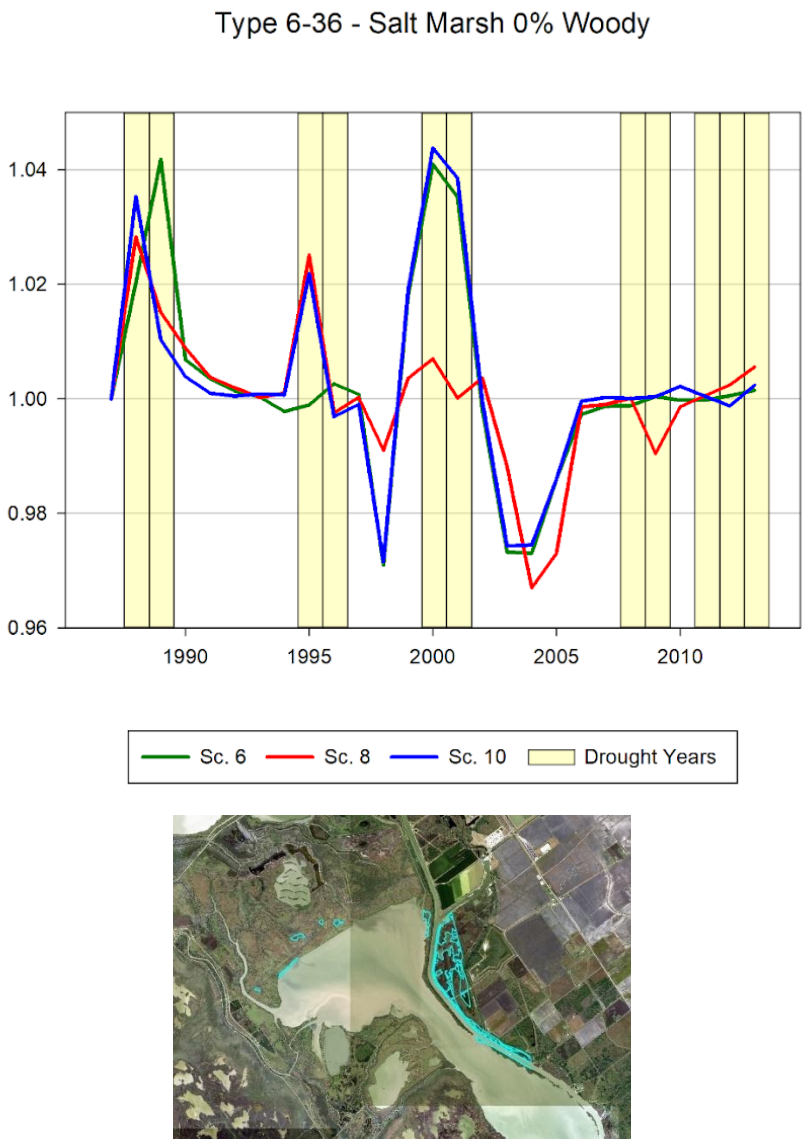

Figure B-4. Total aboveground biomass response for salt marsh, 0 percent woody community for scenarios 6, 8, and 10 (top) and location of this plant community (bottom)

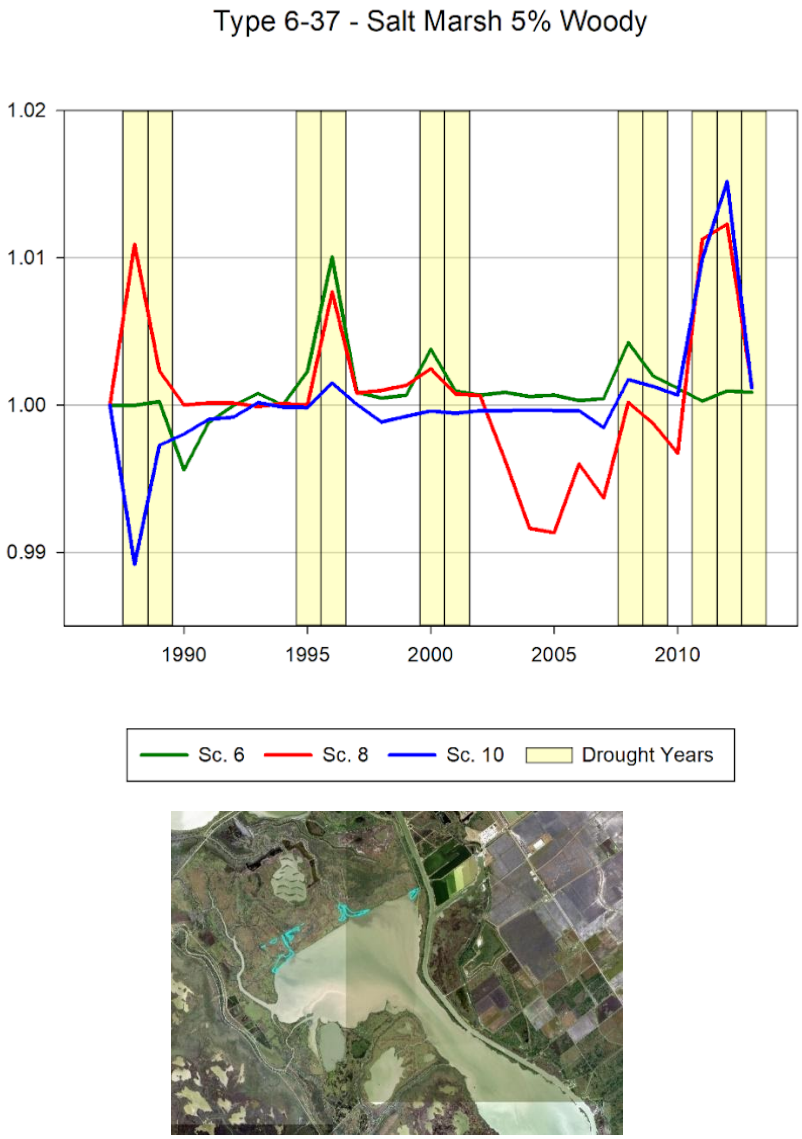

Figure B-5. Total aboveground biomass response for salt marsh, 5 percent woody community for scenarios 6, 8, and 10 (top) and location of this plant community (bottom)

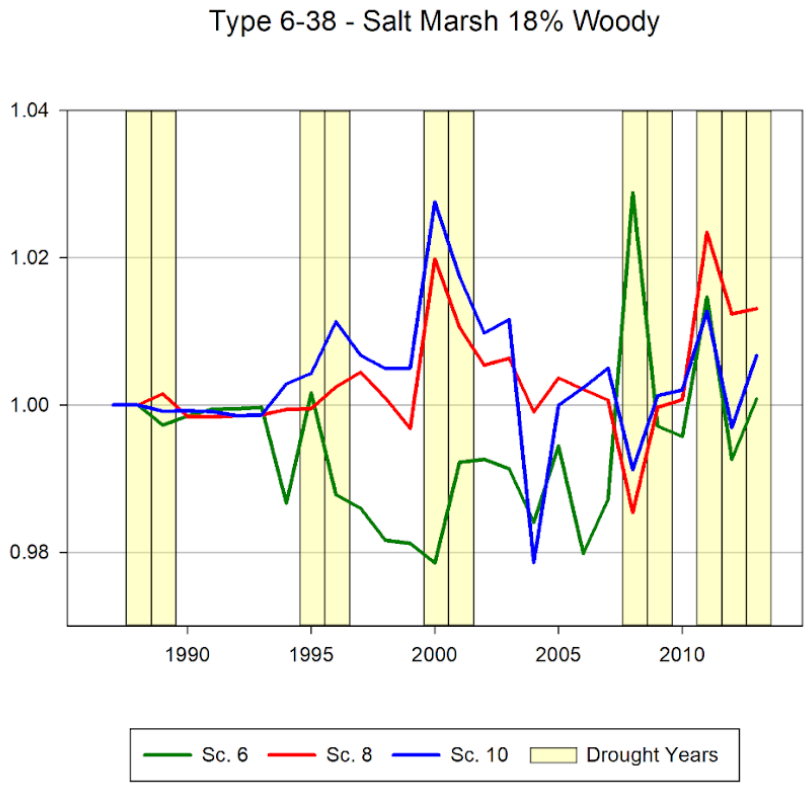

Figure B-6. Total aboveground biomass response for salt marsh, 18 percent woody community for scenarios 6, 8, and 10 (top) and location of this plant community (bottom)

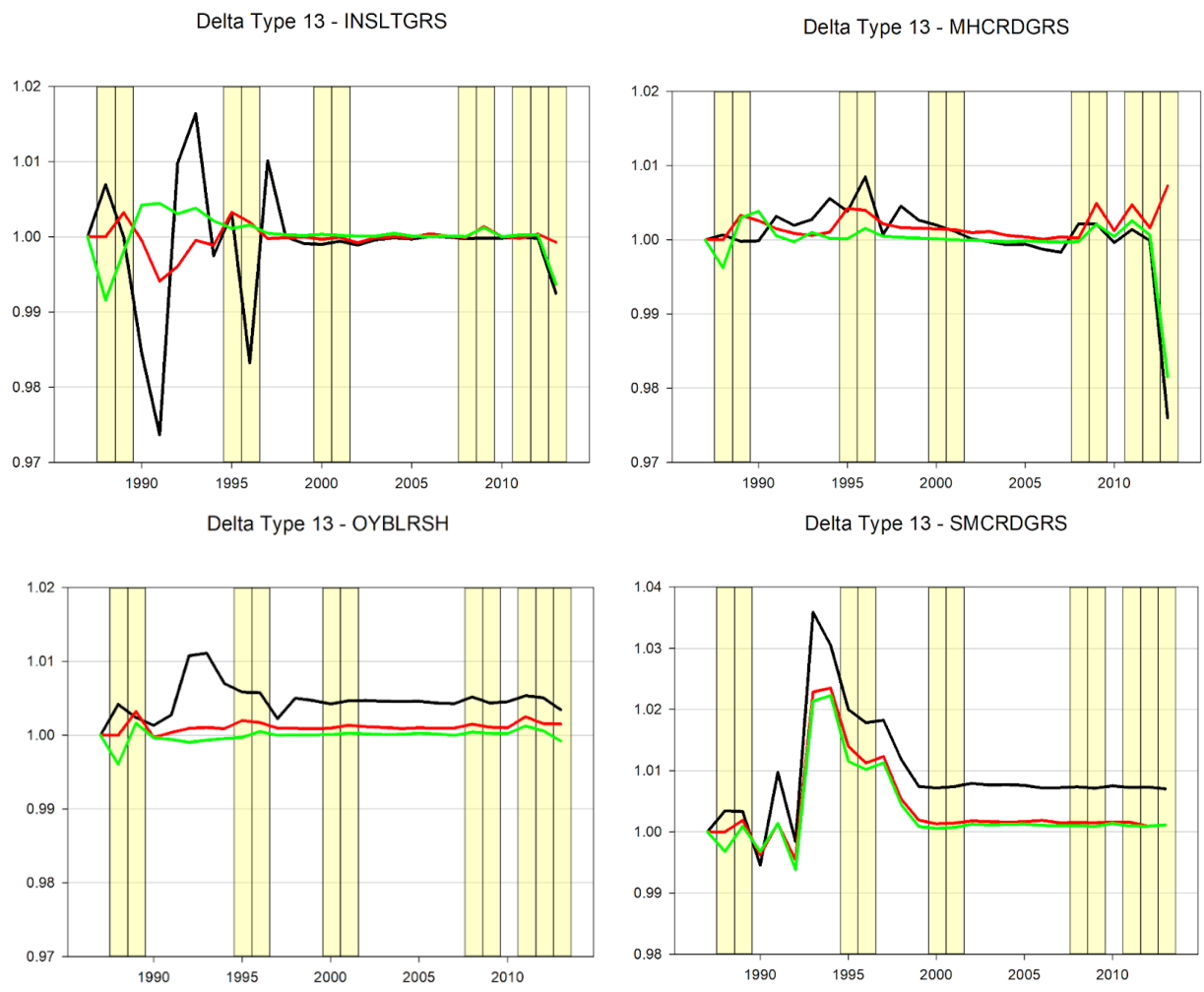

Figure B-7. Total aboveground biomass response for salt marsh, 0 percent woody community for inland saltgrass, marshhay cordgrass, Olney bulrush, and smooth cordgrass for scenarios 6 (green), 8 (red), and 10 (black), location of this plant community is shown Figure B-1

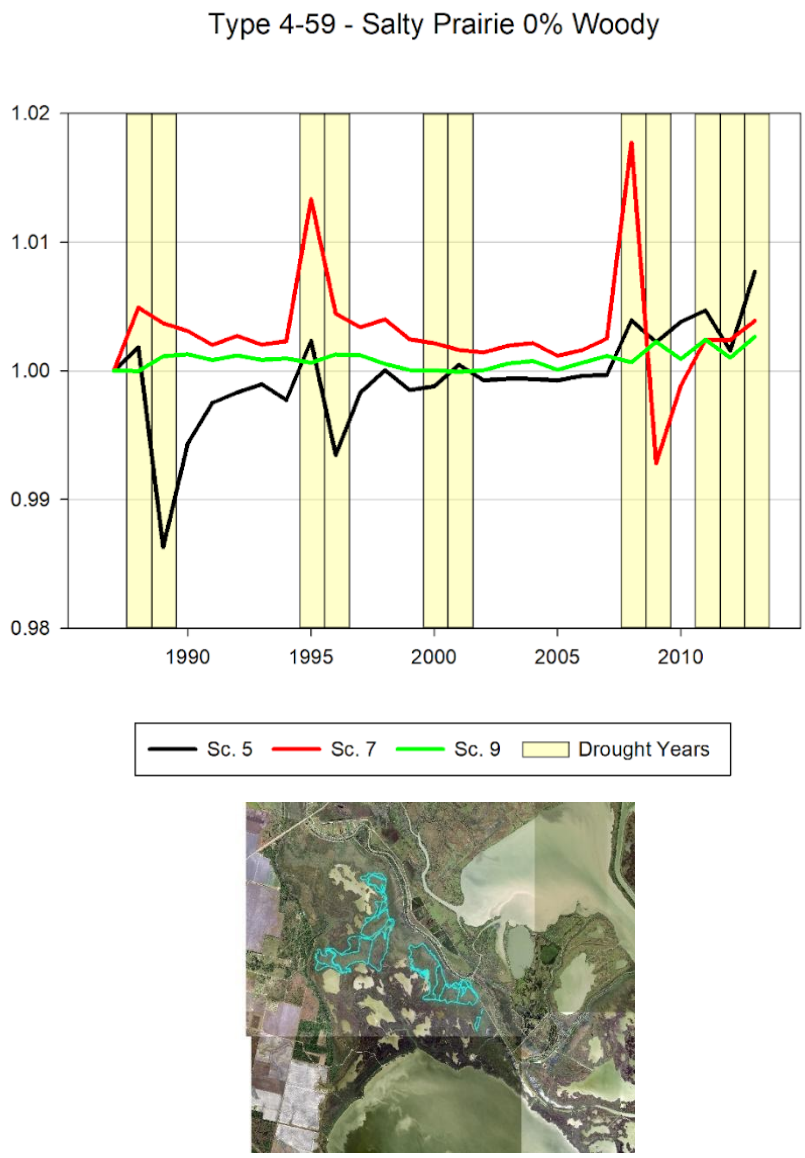

Figure B-8. Total aboveground biomass response for salty prairie, 0 percent woody community for scenarios 5, 7, and 9 (top) and location of this plant community (bottom)

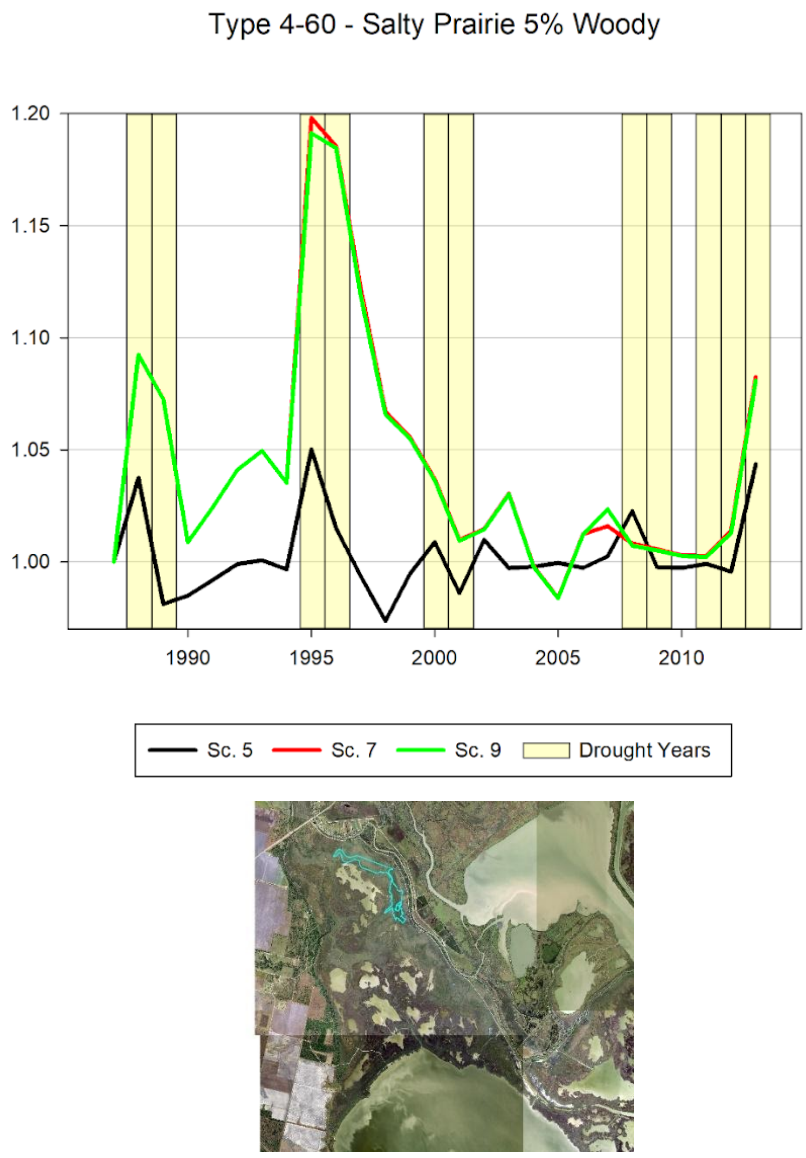

Figure B-9. Total aboveground biomass response for salty prairie, 5 percent woody community for scenarios 5, 7, and 9 (top) and location of this plant community (bottom)

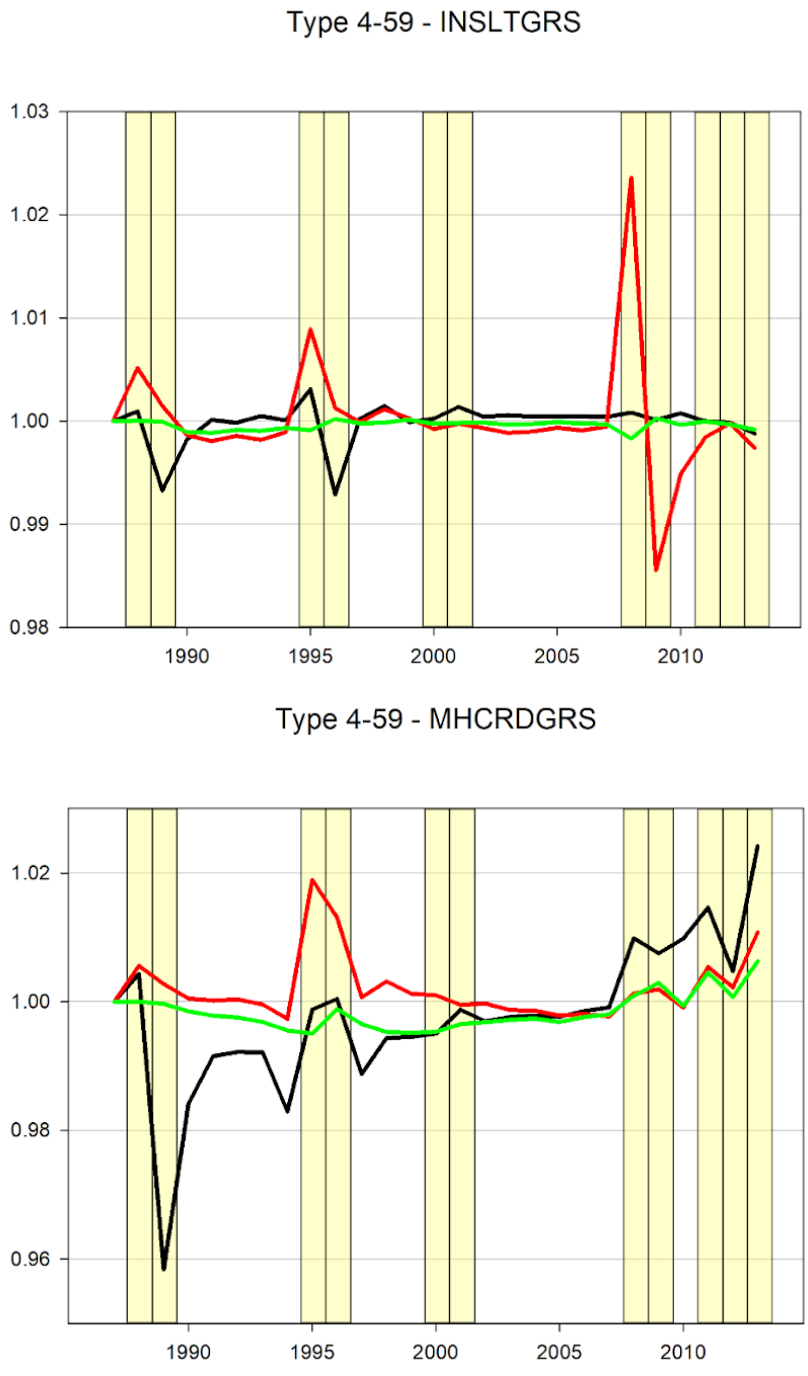

Figure B-10. Total aboveground biomass response for salty prairie, 0 percent woody community for inland saltgrass and marshhay cordgrass for scenarios 5 (black), 7 (red), and 9 (green), location of this plant community is shown Figure B-8

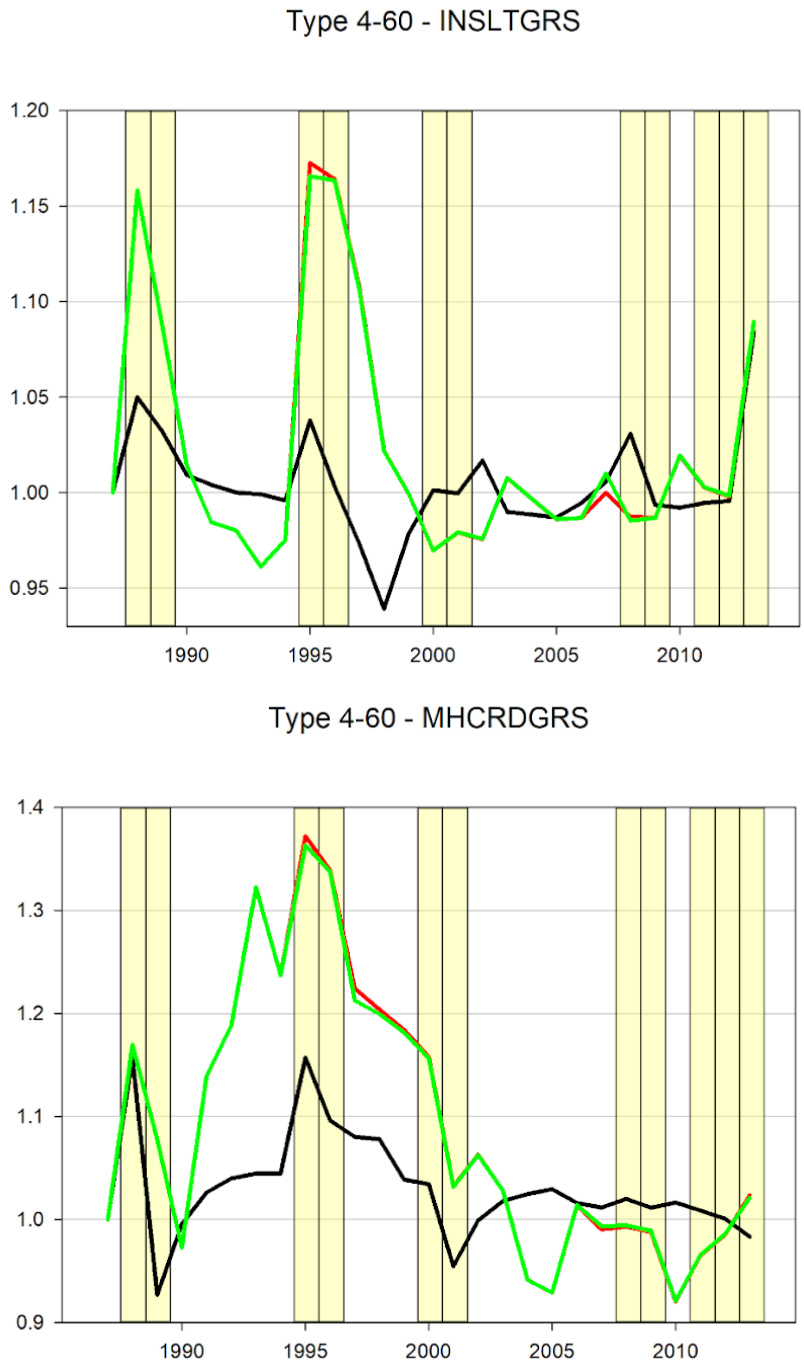

Figure B-11. Total aboveground biomass response for salty prairie, 5 percent woody community for inland saltgrass and marshhay cordgrass for scenarios 5 (black), 7 (red), and 9 (green), location of this plant community is shown Figure B-9

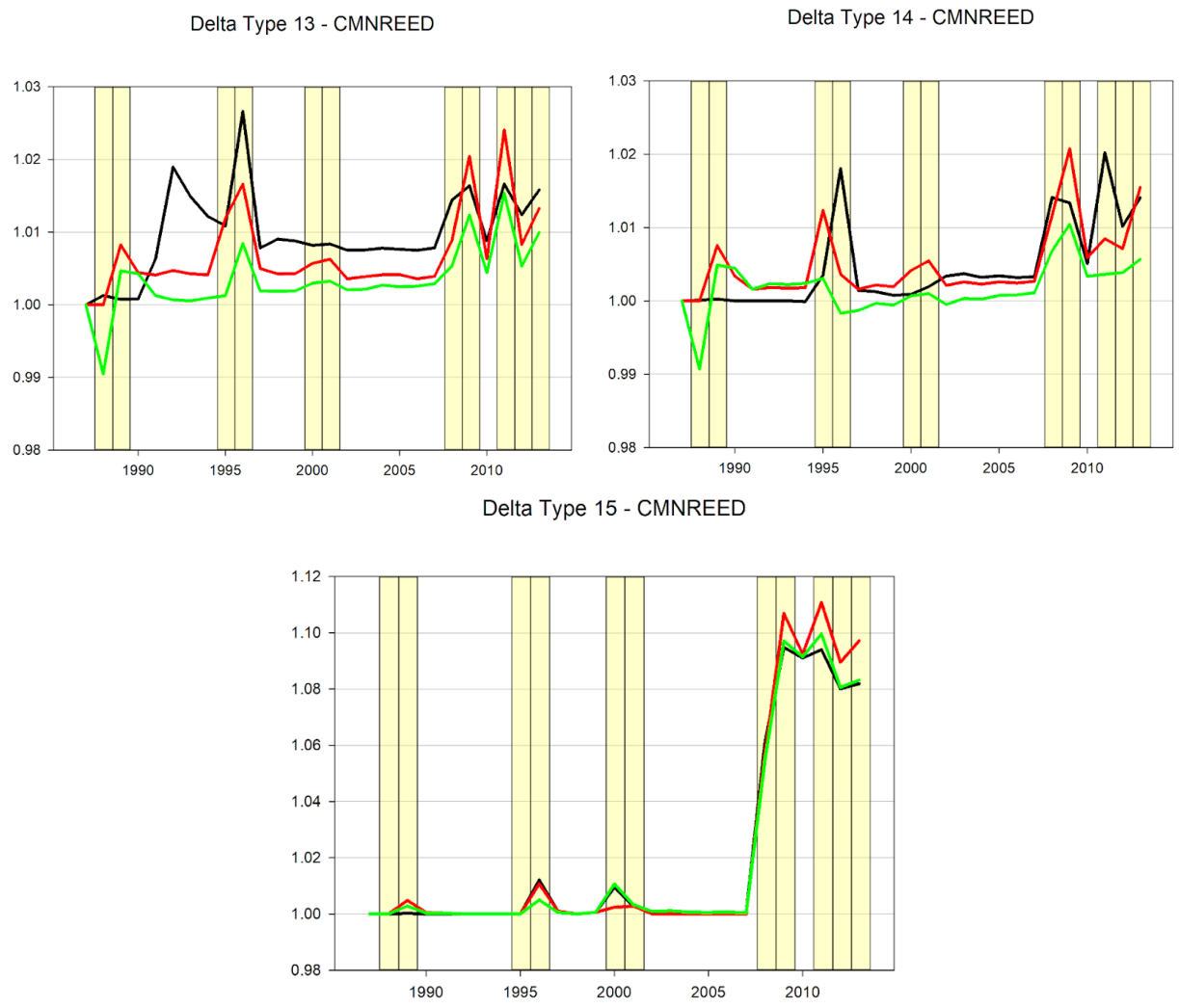

Figure B-12. Total aboveground biomass response for common reed in salt marsh communities on Mission Lake for scenarios 6 (green), 8 (red), and 10 (black), locations of these plant communities are shown Figures B-1 through B-3